NTNU – Trondheim
Norwegian University of
Science and Technology

Jet Pump

Fredrik Liknes

Petroleum Geoscience and Engineering
Submission date: June 2013
Supervisor: Harald Arne Asheim, IPT

Norwegian University of Science and Technology
Department of Petroleum Engineering and Applied Geophysics

NORWEGIAN UNIVERSITY OF SCIENCE AND TECHNOLOGY

Abstract

Faculty of Engineering Science and Technology
Department of Petroleum Engineering and Applied Geophysics

Master of Science

Jet Pump

by Fredrik Liknes

In this Master Thesis jet pumps have been reviewed. Jet pumps are considered as a higher volume artificial lift method and operates by passing a high-pressure fluid jet through a venturi system. Cunningham's equations on jet pumps have been chosen to present the jet pump fluid mechanics.

Factors impacting the jet pump performance have been investigated through a verified model. The performance of Prosper has been compared to Cunningham's model. A self-built model has been developed to calculate a well with a jet pump installed. An optimization has been performed on selected values to find the optimum combination of these.

Jet pump performance and efficiency is dependent on several factors, such as: loss coefficients, densities, geometrical configurations, depth location, injection rate and pressure. These factors influence on performance have been studied.

A comparison of Prosper's jet pump model with Cunningham's showed a discrepancy which was believed to be related to the jet pump implementation in Prosper.

A self-built model was implemented to calculate a jet pump installed well. Some parameters were varied to investigate changes in production. Based on these results an optimization was suggested. By installing a jet pump the optimum results showed a 47% increase for the optimized pump compared with the well without jet pump installed.

NORGES TEKNISK-NATURVITENSKAPELIGE UNIVERSITET

Abstrakt

Fakultet for Ingeniørvitenskap og teknologi
Institutt for Petroleumsteknologi og anvendt geofysikk

Master i teknologi

Jet Pump

av Fredrik Liknes

I denne masteroppgaven er jetpumper undersøkt. Jetpumper er kategorisert som et høyvolums kunstig løft-alternativ og drives av en høytrykks fluidjet som strømmer gjennom et venturisystem.

Gjennom en verifisert modell har jetpumpens ytelse blitt undersøkt. Prospers ytelse har blitt sammenlignet med Cunninghams jetpumpemodell. En egenutviklet modell for beregning av oppnåelige rater med jetpumper installert har blitt utviklet. En optimalisering har også blitt gjennomført på utvalgte parametre for å finne den optimale kombinasjonen av disse.

Jetpumpeytelse og effektivitet er avhengig av flere faktorer, som: tapskoeffisienter, tettheter, geometriske konfigurasjoner, dybdeplassering, injeksjons-rate og trykk. Disse egenskapene har blitt undersøkt nærmere i oppgaven.

En sammenligning av Prospers jetpumpemodell med Cunninghams modell viste en uoverenstemmelse som antas å være på grunn av jetpumpeimplementasjonen i Prosper.

Den egenutvikle jetpumpemodellen ble brukt for å beregne mulig produksjon med jetpumpe installert. Noen parametre ble valgt for å gjennomføre en sensitivitets-analyse. Basert på disse resultatene ble en optimalisering foreslått. Ved å installere en optimal jetpumpe viste beregningene en økning i rate på 47% sammenlignet med en brønn uten noen form for kunstig løft.

Preface

This thesis is written in the fulfilment of Master of Science through the course 'TPG4905 - Petroleum Production, Master Thesis' at the Norwegian University of Science and Technology (NTNU). The title is 'Jet Pump' and the thesis is written by Fredrik Liknes. Where work or publications from others are referred to, or help and guidance has been given, this is clearly stated. The thesis is written in co-operation with professor Harald Arne Asheim and Statoil, represented by Gisle Otto Eikrem, Geir Heggum and Torstein Vinge. The thesis is handed in with gratitude to the above-mentioned supervisors.

A specialization project on jet pumps was carried out in the autumn of 2012. This project raised new questions regarding jet pumps and it was decided it would be interesting to carry out a Master on the subject. Especially a jet pump in communication with a well would be interesting to investigate further.

Jet pump is a high volume artificial lift alternative. The pump utilizes a high flow jet to transfer energy in a venturi system. The jet pump is singled out because of its robust and simple design. The theory behind jet pumps is thoroughly described. There exist a number of black box models to calculate jet pump performance. One goal of this thesis was to understand one of these better. A self-built model was developed as well to calculate a specific well. Optimization on selected variables where also completed in order to find the best-suited pump among a range of values.

Contents

Chapter 1

Introduction

Jet pumps are downhole pumps used to improve production from declining wells. Jet pumps are interesting because of their robust design and capacity for lifting large volumes of fluid. In this context it is important to verify jet pump performance and assess influencing factors. Understanding and establishing a trusted tool to calculate performance is also important to consider jet pumps as an artificial lift alternative. The following items were listed as goals for this thesis.

- Define an optimal jet pump design and describe the variables that can be adjusted and the process constraints.
- Model a jet pump in Prosper based on the theoretical model
- Compare results from Prosper with the jet pump model.
- Optimize jet pump design for a given well by use of the automation framework.

To answer these questions a search in literature was carried out to find field experience and theoretical work on jet pumps. Thereafter, a computer model was built based on theory found in literature. The model was applied on a specific well to compare performance with Prosper's jet pump module. An optimization was performed to automate the jet pump selection procedure among the selected optimization variables.

Chapter 2

Jet Pump Theory

2.1 The Jet Pump

Jet pumps are simple devices, as shown in Figure 2.1. A jet pump consists of four static parts: nozzle, throat inlet, throat and diffuser. Highly pressurized power fluid is converted to kinetic energy through the nozzle. Reservoir fluid, with a much lower pressure, is accelerated into the throat. The fluids are mixed in throat and a homogeneous mixture is developed at diffuser inlet. The combined fluids kinetic energy is converted to pressure energy in the diffuser. The pressure increase across the pump lifts the mixture to the surface.

Fundamental theory derived by Cunningham in the Pump Handbook[1] is used to describe the fluid mechanics. Each part of a jet pump has its own flow regime with corresponding equations to express how pressure and other properties change through the jet pump. These equations are presented in Appendix A.

The energy increase across the jet pump can be seen in Figure 2.2. This figure can be understood as experienced well pressures. The left line shows the pressure change in tubing from reservoir to throat-entry. The natural reservoir energy is not capable of lifting the desired reservoir rate to surface. The right hand line shows the experienced pressure in annulus as injection pressure is exerted on the hydrostatic column. The energy exchange across the jet pump provides sufficient energy to lift the combined fluids to surface. The diffuser pressure is located between suction and the nozzle injection pressure.

As for any pump, the efficiency of a jet pump is described as:

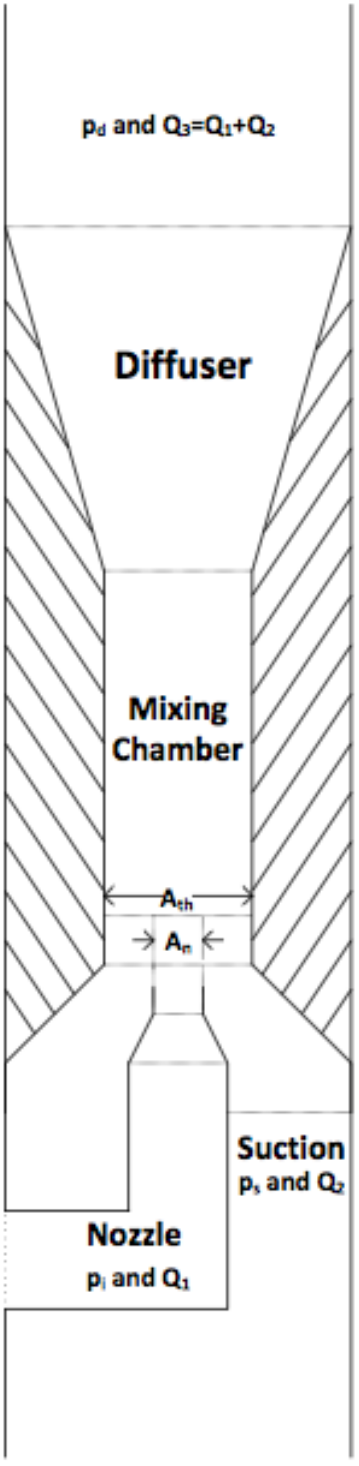

FIGURE 2.1: Jet Pump Sketch

$$\eta_{pump} = \frac{Energy\ Gained}{Energy\ Supplied} \tag{2.1}$$

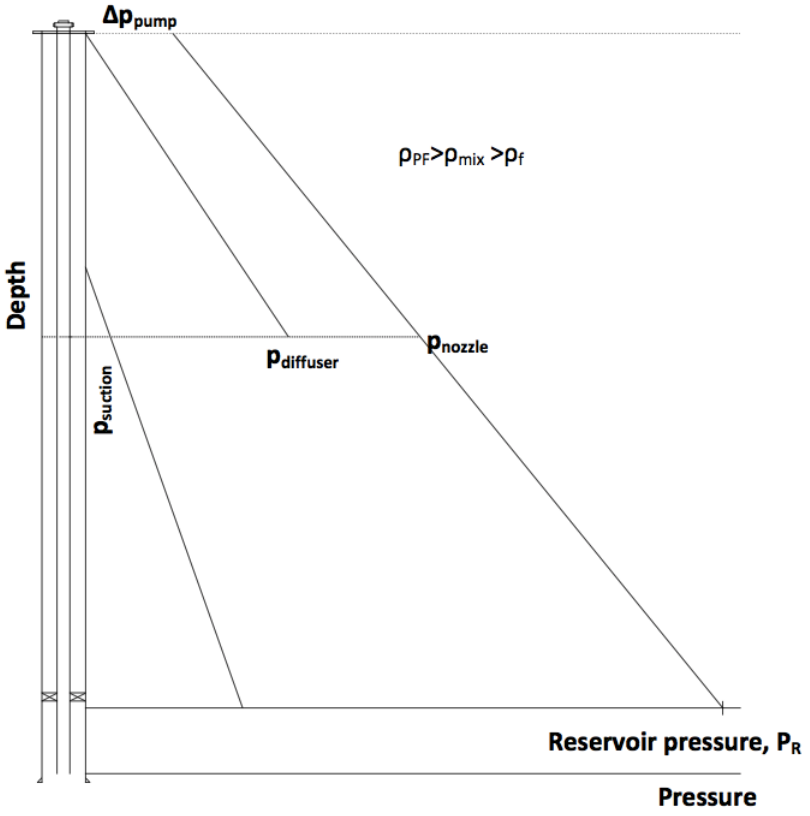

FIGURE 2.2: Well with Jet Pump

Expressing the efficiency through rate and pressure the following equation describes efficiency for given conditions.

$$\eta_{pump} = \frac{(p_{di} - p_s)}{(p_n - p_{di})} \frac{Q_2}{Q_1} \tag{2.2}$$

Pressure increase of reservoir flow to the pressure drawdown of power fluid defines the jet pump efficiency. The energy exchange is seen as pressure variation in the jet pump. Figure 2.3 shows the pressure change in the jet pump both for the reservoir flow and the power fluid flow.

Based on this figure, each part is described with the corresponding flow equations. Necessary design considerations are presented in subsequent sections.

Nozzle

Jet pumps are normally operated in two manners[2].

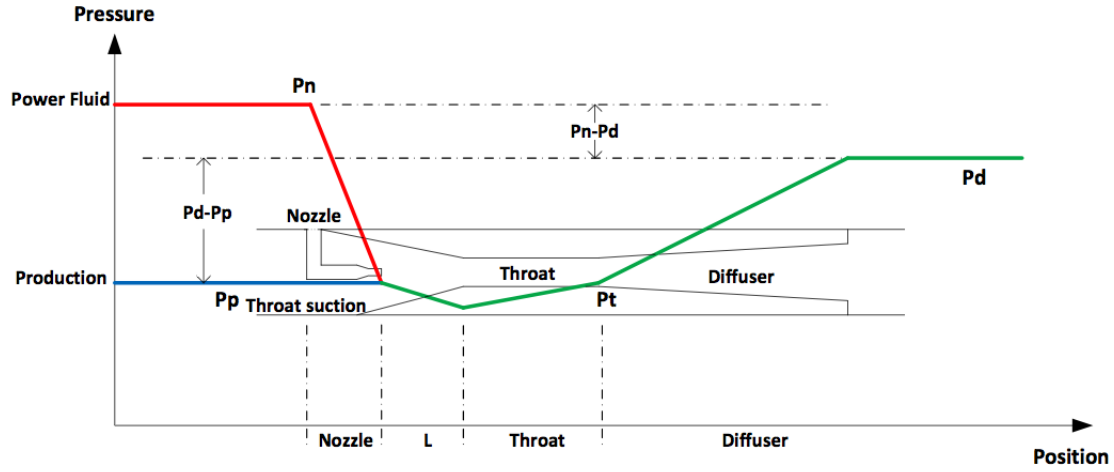

FIGURE 2.3: Jet Pump Pressure Trend

- *Reversed Fluid Circulation*: Power fluid is pumped through annulus and commingled fluids are produced through tubing.
- *Forward Fluid Circulation*: Power fluid is pumped through annulus and commingled fluids are produced through annulus.

In either case the driving energy added from the power fluid is composed of kinetic energy and potential energy. The kinetic energy relates to circulation rate and the potential energy from nozzle-entry pressure. Power fluid has been pumped through annulus and arrives at jet pump depth with both kinetic and potential energy. Power fluid enters the jet pump through a nozzle. This flow restriction causes a decrease in pressure as potential energy is transferred to kinetic energy. The power fluid flowing through the nozzle, discharge in throat as a high velocity jet. In throat-inlet the power fluid is mixed with reservoir fluid.

In section 2.3 necessary considerations in designing the nozzle is presented.

Throat-entry

Reservoir fluid is produced through tubing and the fluid properties along with pressure and temperature changes along the flowpath. The reservoir fluid enters the jet pump through throat-entry. This area is the annular space between the jet pump wall and nozzle. The reservoir fluids flow into the pump due to a lowering of pressure in throat-inlet, as shown in Figure 2.3. This pressure drawdown is created by power fluid jet suction.

The mixing of the two fluids start instantaneously[3] and the energy exchange begins when these flows meet. The necessary considerations in designing the throat-entry are not as extensive as for the other parts, and is presented in Section 2.4.

Throat

The main energy exchange happens in throat where the two fluids mix. The assumption is that the fluids are completely mixed at throat outlet. Both the flows entering and the mixed flow exiting are assumed to have uniform velocity distributions. The momentum balance equation is applied based on this assumption. This implies that the momentum of the combined fluids at throat outlet equals the momentum of the fluids entering the throat[4]. Throat considerations are presented in Section 2.5.

At throat outlet the mixed fluids have high kinetic energy and a diffuser is necessary to exchange this to potential energy.

Diffuser

Âă

The diffuser is a conical tube that expands from the throat barrel to the inner diameter of the tubing. The diffuser length determines the jet pump pressure recovery. A gentle diffuser angle offers a better pressure recovery. At diffuser outlet a lot of the kinetic energy is exchanged to potential energy. This increase in potential energy offers the necessary energy to lift the combined fluids to surface. Diffuser considerations are given in Section 2.6.

2.2 Jet Pump Installed Well

A jet pump is an integral part of a production well and the whole system is shown in Figure 2.4. The system consists of injection pump, injection valve, jet pump, processing facilities, production packers, safety valve and wellhead. This section describes the main parts that are relevant for this thesis. In a real system the number of components is higher.

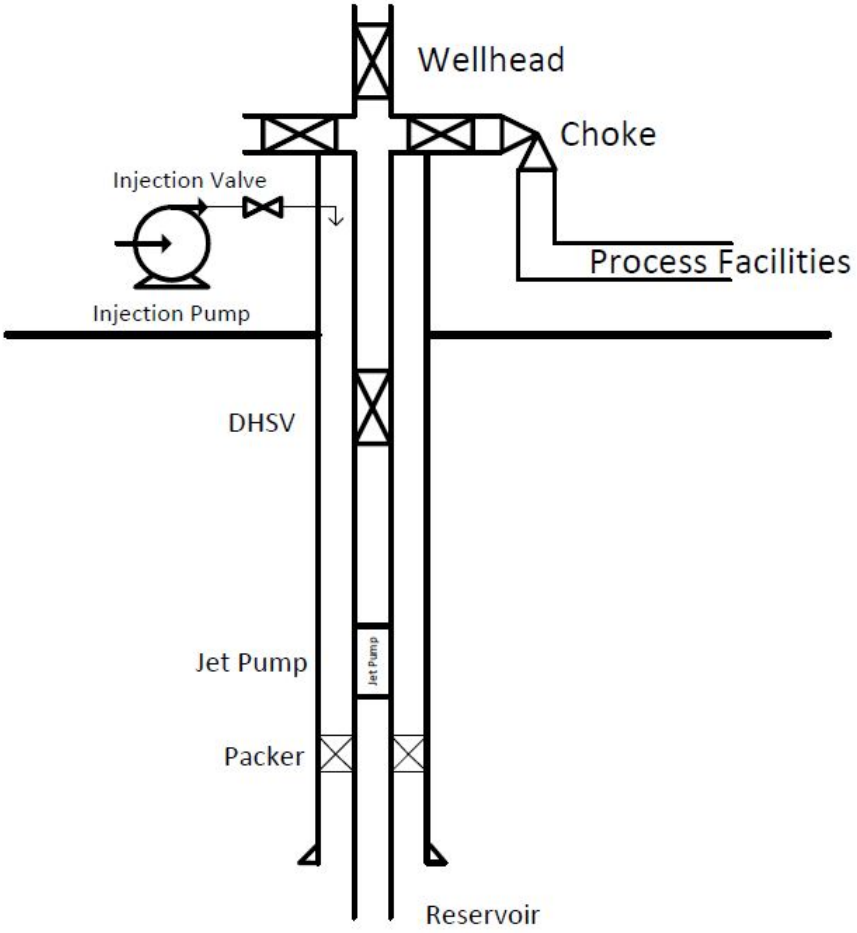

FIGURE 2.4: Jet Pump Well with Main Components

Power fluid is pressurized at surface by an injection pump and the power fluid is injected through the annular injection valve at wellhead. From this valve the fluid is transported through annulus. The wellhead is designed to withstand maximum expected well pressures to occur, and exceeding this design pressure could damage the well. The applied driving pressure from surface propagates downhole and increases the annular pressure down to the first annular seal. An annulus seal is a restriction that prevents fluids from flowing by. If such seals are installed the jet pump location has to be above these in order to transport power fluid to nozzle inlet.

The natural reservoir energy lifts the reservoir fluids to jet pump suction. Above a jet pump the commingled fluids are produced to surface. Energy added through power fluid provides sufficient lift to meet the required wellhead pressure. Towards surface there is a Downhole Safety Valve (DHSV) that provides a barrier. The safety valve is operated from surface and can seal the well if leakage is detected.

Field Applications

Three cases are included in Appendix C. They contribute to demonstrate how jet pumps are applied to date. Jet pumps were developed in the nineteenth century and have been described as a reliable artificial lift method. Jet pumps are said to be redundant compared to other methods. Table 2.1 list reported uptimes for field installed jet pumps.

Table 2.1: Reported Uptimes for Field Installed Jet Pumps

Operator	**Location**	**Field**	**Run time (Years)**	**Well**
Marathon	Alaska	McArthur River	2	D-4RO
Tenneco	GoM	Main Pass	1.5	A5
AGIP	Italy	Vega	2	3 Off
Lundin	Tunisia	Oudna	5.3	1
BP	UK	Thistle	0.9	A51
Shell	UK	Auk	2	Several

The aforementioned uptimes are less than what a isolated jet pump may withstand. The other system parts have a shorter lifetime compared to a jet pump. The system, were the jet pump is connected to other parts, thus have a shorter lifetime.

Jet pumps are known for their low efficiency compared to other artificial lift methods. However, other benefits of using jet pumps might compensate for the reduced efficiency, such as:

- Âă*Lifetime:* Expected lifetime of lift method might favor using a less efficient method.
- *Uptime:* If rapid downtimes are encountered, this might affect the choice
- *Economy:* Operational costs of running the artificial lift method. Acquisition costs might also influence the selection.
- *Safety:* Safety considerations could exclude certain methods.
- Âă*Pressure:* Necessary backpressure might change for the various methods.

In the subsequent sections, considerations of the various parts are listed.

2.3 Nozzle Considerations

Changing the nozzle diameter will affect jet and nozzle behaviour. The kinetic energy created in nozzle as the pressure is drawn down is dependent on nozzle diameter. From equation 2.3 it is evident that nozzle velocity is inversely proportional with the nozzle diameter.

$$v_n^2 = \left(\frac{Q_1}{A_n}\right) = \frac{2\Delta p}{\rho_1(1+K_n)} \tag{2.3}$$

A problem occurs if the velocity in throat inlet approaches the speed of sound. This state is referred to as Mach Number 1, $Ma_o = 1$[1]. The Mach Number is defined as the object speed relative to the speed of sound[5].

$$Mach\ Number = Ma = \frac{Object\ Speed}{Speed\ of\ Sound} \tag{2.4}$$

If this state is reached, the flowing velocity is equal to the speed of sound in the fluid. Any further increase in pump rate will not affect jet pump performance. As for an aeroplane travelling at the speed of sound, the jet pump will also experience shock waves due to fluid compressibility. Fluid compressibility could especially be a problem in cases with high Water-Cuts. Water compressibility could cause fluid hammer effects, which could possibly damage the jet pump material.

Several experiments have been carried out on the geometrical shapes. The purpose was to investigate if changing nozzle shapes could improve efficiency. Winoto, Li and Shah[6] tried with non-circular nozzles such as squared and triangular. Results from this study showed that all configurations had lower efficiency compared to the circular shaped.

2.4 Throat-Entry Considerations

Throat has to be shaped in a way that limits frictional losses as the reservoir fluid passes through into the throat. A rounded entry will guide the reservoir fluid into throat without inducing too much turbulence[1], thus reducing friction. Higher losses are experienced if the throat-entry is not shaped correctly[7].

2.5 Throat Considerations

The power fluid is mixed with reservoir fluid in throat. It is assumed that the fluids enter throat with uniform velocity profile[1]. The criteria for proper throat length are that it should be sufficiently long to accomplish the mixing of the two fluids. Likewise, it should be short enough to limit frictional losses. The one-dimensional theory does not include lengths of the different sections, which make it difficult to quantify throat lengths through mathematical expressions. The power fluid jet length will also be dependent on the size of nozzle and pump rate. Throat length should be sufficiently long in order to avoid the jet ending in diffuser.

For a water jet-pump, El-Sawaf et al.[8] reports that an optimum throat length is $7.25D_{th}$ over a $6.75D_{th}$ and $7.86D_{th}$ configuration for the specific conditions carried out in their project. According to Prabkeao and Aoki[9], the throat length decreases as the nozzle-throat ratio increases. The mixing throat length also increases as the flow-ratio decreases and the nozzle location is closer to throat entrance.

Cunningham and Dopkin[10] suggest that an optimum throat length can be determined from the following expression.

$$\Big(\frac{d_n}{L_{th}}\Big)_{optimum} = 15\Big(\frac{A_{th}}{A_n} - 1\Big) \tag{2.5}$$

Cunningham[1] recommends, in a later publication, a mixing throat length of $6D_{th}$. Literature indicates that a throat length should be chosen by trail and error by using several different throat lengths. However, a throat in the range $8 - 10D_{th}$ seems appropriate.

Cavitation

Cavitation could also prove to be a problem with jet pumps. Cavitation occurs when throat-inlet pressure drops beneath the vapour pressure. Typically, cavitation is a problem when too much fluid is forced through the throat area[11]. Power fluid cavitation is also a possibility, and occurs if there is too little production. When cavitation occurs, any further decrease in backpressure has no effect on

flow-ratio. Cavitation may also contribute to the deterioration of the pumps, as bubbles implode and shockwaves hit the jet pump wall.

Bonnington and King[12] and Cunningham and Hansen[13] suggest that the following criteria should be used to find the limit for the flow-ratio, and that the operating flow-ratio should be somewhat below this.

$$M_L = c\sqrt{\frac{p_s - p_v}{\sigma Z}} \tag{2.6}$$

Where σ is the cavitation coefficient, suggested to be 1.35[13].

In an oil well application the well pressures are much higher than the vapour pressure of water. This implies that cavitation is not a problem as long as the installation depth is sufficient to locate the throat-inlet pressure above the vapour pressure[14]. If the throat-inlet operating point is below the boiling point curve of water, shown in Figure 2.5, cavitation is avoided.

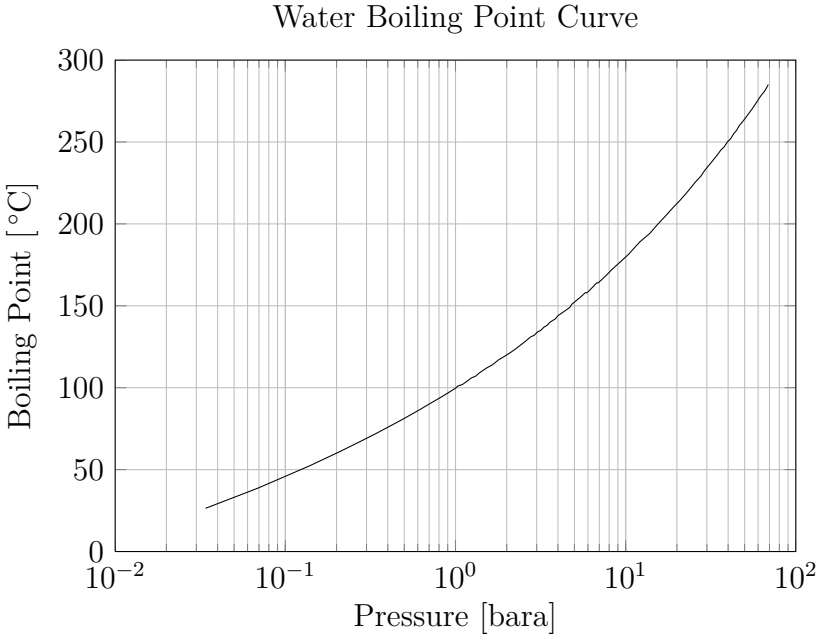

FIGURE 2.5: Water Boiling Point Curve

2.6 Diffuser Considerations

The diffuser converts kinetic energy into potential energy. The length and angle of diffuser is difficult to quantify without experiments. One-dimensional theory

does not include longitudinal dimensions, which make it difficult to express this qualitative. However, certain publications suggest a diffuser angle of 3.6°. Teamia et al.[15] suggests a diffuser angle of 5.5°. Cunningham[1] defines the relationship between throat and diffuser area as a, and it can be written mathematically as:

$$a = \frac{A_{th}}{A_d} \tag{2.7}$$

2.7 Power Fluid Considerations

The efficiency improves as the amount of dissolved gas increases. Kumar, Telang and De[16] report, for the offshore NLM field west of India, that using sea water as power-fluid was successful. A small sacrifice in efficiency was experienced. Riva et al.[17] used Naphta in their Vega and Gela fields, and reported an improvement in mixing capabilities along with improved well dynamics.The choice of power fluid is a trade-off between several issues listed in Table 2.2.

Table 2.2: Power Fluid Considerations

Oil	**Water**
Less hydrostatic pressure up- and downstream	Fluid hammer effects
Reduced viscous forces	EmulsionsÂă
Lubrication qualities	Corrosion (sea-water)
	Unlimited supply
	Improved efficiency

Compatibility must also be considered. If power fluid is not compatible with the reservoir fluid this may form permanent emulsions that require challenging separations at surface. Power fluids capable of transporting dissolved gas must also be considered.

2.8 Friction Factors

There are frictional losses associated with all parts of a jet pump. These loss coefficients are dependent on area, viscous losses, mixing related losses and flow rates. Suggested loss coefficients vary and frictional losses are dependent on the

specific pump used. Hatziavramidis[18] states that constant value loss coefficients are valid for a specific range of nozzle-throat-area ratios. Constant value loss coefficients are also likely in cases with high Reynolds Numbers.

Mikhail and Abdou[19] suggest an experimental loss coefficient expression based on Reynolds Number. Equation 2.8 is suited for jet pump-parts that are subjected to high velocity flow, such as nozzle and throat. It should be noted that the numbers in equation 2.8 are case dependent (viscosity, density etc.).

$$K_i = \frac{379}{Re^{0.63}} \tag{2.8}$$

Wærp[7] found in his experimental Master Thesis on jet pumps, that equation 2.8 gave approximately similar results between modelled and experimental values for specific jet pump configurations. A plot of Loss Coefficients calculated with equation 2.8 against Reynolds Numbers are shown in Figure 2.6.

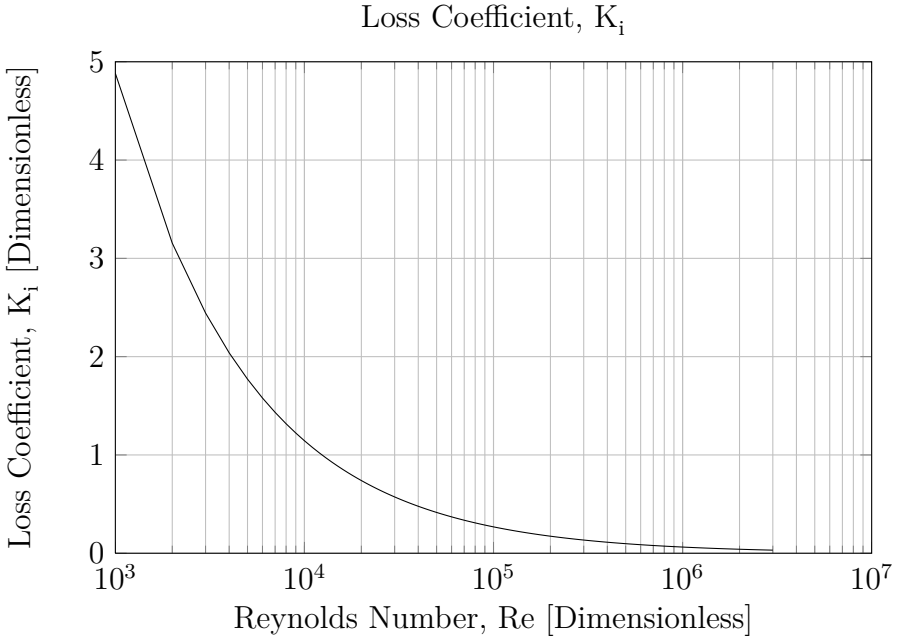

FIGURE 2.6: Loss Coefficients, K_i

The flowing velocity in the various jet pump parts favours constant-value loss coefficients. Many authors have suggested appropriate loss coefficients that suited their specific jet pump. In Table 2.3 the suggested loss coefficients by different authors are summarized.

TABLE 2.3: Reported Loss Coefficients from Literature

Author	K_{en}	K_n	K_{th}	K_{di}	K_{td}
Gosline	0	0.15	0.28	0.10	0.38
Petrie et al.	0	0.03	N/A	N/A	0.20
Cunningham (minimum values)	0	0.10	N/A	N/A	0.30
Sanger	0.036	0.14	0.102	0.102	N/A
	0.008	0.09	0.098	0.102	N/A
PTC	0.05	0.03	0.1	0.1	N/A
IPM	0	0.15	0.28	0.10	N/A

The loss coefficients are also area dependent, and will have different values for varying areas. This implies that the values presented in Table 2.3 are only valid for a range of R-values.

2.9 Prosper Jet Pump Implementation

The jet pump implemented in Prosper[20] is compared with Cunningham's model. To understand how they behave it is important to know about Prosper and the theoretical framework it is built on.

Prosper is a program used to model, design and optimize well performance. The program assist a production engineer or reservoir engineer in these processes. The program calculate well hydraulics and other well properties that are subjected to changes in the wellbore.

The program is also capable of modelling various artificial lift alternatives, such as Gas Lift, ESP and Jet Pumps. The different modules may be used to verify performance and perform sensitivity analysis for changing conditions.

The jet pump module is based on the work by Brown[21] and Hatziavramidis[18]. The equations describing the energy exchange is based on the total energy losses. Cunningham use energy balance equations. In his model, throat-inlet, nozzle and diffuser is described by the Bernoulli's energy conservation and throat by the momentum balance equation.

2.10 Short on Optimization

An optimization algorithm seeks to find a solution that best fit a data set or satisfy some formulated equality. The optimization algorithm used in this Master is quite similar to the solvers described in Chapter 3. One difference between a solver and an optimization algorithm are the number of objectives. A solver is a single objective optimization[22] seeking a solution along a line of values within the range envelope. Multi-objective optimization finds a solution over several parameters. Hence, there are several input parameters that can be tuned to affect performance to fulfil some convergence criteria. This often implies that there exists a trade-off between several parameters. In this case, a solution exists when the objective function has taken a minimum value in this case.

To find a solution that is a global minimum can be challenging. The optimization algorithm may find an optimum that seems to be the correct answer based on nearby results. But, this may be a local minimum, and not a global minimum. Choosing initial values close to the probable result is beneficial because the solution found is likely to be the correct one. Also, the computation time will probably be less because the starting point is quite close to the actual solution.

The optimization tool used in this Master Thesis is an open source code called IPOPT. The development project is led by Wächter and Vigerske[23] and the software package is meant for large-scale non-linear optimization. The Interior Point Optimizer (IPOPT) utilizes an interior-point algorithm, and is built on the idea that any convex problem can be formulated as finding the maximum or minimum of a objective function. In our case this implies minimizing the object function by varying the selected optimization variables.

The solver used in Section 3.3 use Automatic Differentiation (AD) to differentiate the function. In optimization problems the function is often not possible to differentiate and numerical derivation is thus necessary to solve the problem. This is done by perturbation in the vicinity of the evaluated function and the change in gradient in the tangent plane is evaluated. The gradient in each point is calculated by approximation because the derivative of the function is complicated to express explicitly. By using the definition of the derivative, the gradient may be approximated numerically.

$$\frac{\delta f}{\delta x} = \frac{f(x_{i+1}) - f(x_{i-1})}{x_{i+1} - x_{i-1}} \tag{2.9}$$

Where x is one of the variables listed in Table 3.4 and $f(x)$ the calculated reservoir rate, Q_2. The three other parameters are kept constant in turn. This means that for each gradient calculation there are two model executions to perform the calculations. Combined with the 16 computations necessary to calculate the Hessian matrix, the optimization algorithm requires large computation time and power. The routine uses this to select the likely road to obtain convergence.

The second derivative matrix is calculated to know how the function changes along the different variables. It is called the Hessian Matrix and describes the function curvature for every variable. For every gradient calculated it is necessary to calculate the second order derivative with respect to every variable. The second derivatives are not possible to describe explicitly. The Limited-memory reduced-Hessian method is thus used to calculate these[24]. The method is also developed in such a way that it reduces computation time for large problems that require multiple iterations.

In Table 2.4 some optimization variables mentioned in the literature are listed. These parameters can be included in the optimization algorithm to find the optimum jet pump over the specified variables. The principle for multi-variable optimization is the same, independent on number of parameters. The process of including several optimization parameters in the future is therefore manageable.

Table 2.4: Suggested Optimization Parameters from Literature

Parameter	**Publications**
A_n/A_{th}	Andreussi et al.[25]Âă Corteville et al.[26] Jiao, Blais and Schmidt[27]
Q_1	Corteville et al.[26]
p_s	Corteville et al.[26] Cunningham [1]Âă
p_i	Andreussi et al.[25]
Productivity Index (PI)	De Ghetto and Giunta[28] Chavan et al.[29]
Well Depletion	Andreussi et al.[25]
Water-Cut (WC)	Andreussi et al.[25]Âă Chavan et al.[29]
Gas-Oil-Ratio (GOR)	Andreussi et al.[25]Âă Chavan et al.[29]

Chapter 3

Results

3.1 Isolated Jet Pump

The model based on Cunningham's equations was first built in Matlab. The procedure for building and obtaining these results is described in Appendix E.1, with the necessary equations listed in Appendix A.1. To ensure that results were reliable, and that the model was working properly, a set of variables and results were necessary. Expected results based on Cunningham's theory had already been indicated by a Statoil contractor[14] and PTC[30] for a given example well. The first implementation was done for an isolated jet pump. The program took a list of input parameters, presented in Table 3.1, and solved the system. The output from the program was the reservoir rate.

Table 3.1: Matlab Input Parameters

Variable	Description
$a = A_{th}/A_{di}$	area-ratio
A_n	nozzle area
A_{th}	throat area
c	$(1-R)/R$
γ	gas density ratio
K_i	loss coefficient, i=n,en,th,di
p_s	suction pressure
p_i	nozzle injection pressure
p_d	diffuser pressure
Q_1	power fluid injection rate
ρ_1	power fluid density

Equation A.2 was solved first to find the jet dynamic pressure. The three other equations (equation A.7, A.9 and A.11) were thereafter solved simultaneously. The program is briefly summarized in Figure E.1. For further reference see Appendix E.1. When the Matlab program was working properly, the code was converted to C#. The necessary input to the program is described in Appendix E.2. For now, a brief summary follows.

1. Declaration of necessary input variables in a Parameter Dictionary.
2. Define functions and variables (Q_2, p_o and p_t as X, Y, and Z respectively) in a similar fashion as in the Matlab code.
3. First guess of X_o.
4. Specify convergence criteria, number of iterations, maximum step length, content of report, etc..
5. Specify function and Jacobian for evaluations in solver.
6. Run the program with reservoir rate for the given conditions as output.

The Jacobian is calculated by using automatic differentiation[31]. See Appendix E.2 for further information on this differentiation technique. The program was used to study how efficiency changes for selected parameters. The following sections show the sensitivity on parameters discussed in Chapter 2.

3.2 Jet Pump Sensitivity Study

Friction Factors

There are frictional losses associated with all parts of a jet pump. However, there are parts of the jet pump that are more determining to jet pump performance than others. The following results are based on the example well. The incompressible equations, presented in Appendix A.2, are used because of the high Water-Cut. For each plot the other loss coefficients are kept as in the base case. The friction factors are selected based on Table 2.3.

Figure 3.1 shows the change in pump efficiency as the throat-entry loss coefficient is increasing. From this figure it can be seen that there is a negligible decrease in efficiency as the loss coefficient is increasing.

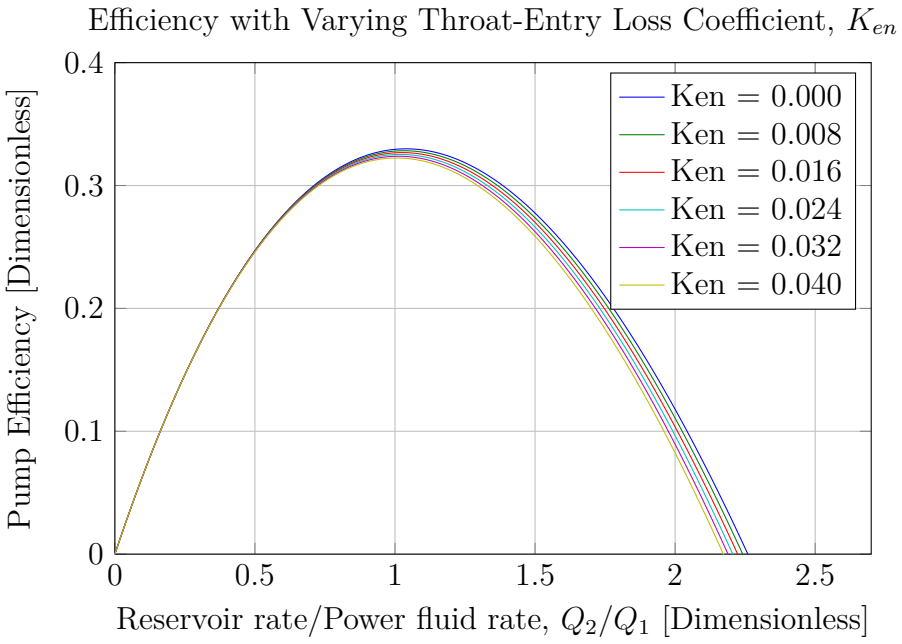

FIGURE 3.1: Efficiency with Varying Throat-Entry Loss Coefficients, K_{en}

The next figure shows pump efficiency for varying nozzle loss coefficients. In nozzle there are high velocities associated as the power fluid flows through the restriction. Figure 3.2 show that the decrease in pump efficiency is somewhat higher for increasing nozzle loss coefficients compared to throat-entry losses. Among the realistic loss coefficients the pump efficiency is about 0.32.

In Figure 3.3 the pump efficiency is plotted for varying throat loss coefficients. The fluids are mixed in throat. Along with high throat velocity, this contributes to increased frictional losses in throat. As the throat loss coefficient is increasing the pump efficiency is dropping rapidly. The optimum flow-ratio is also seen to be decreasing.

Similar behaviour is seen for diffuser. Figure 3.4 shows that increasing diffuser loss coefficients reduce the pump efficiency slightly less than for the throat. For an average loss coefficient of 0.1 the pump efficiency is about 0.33 for a flow-ratio, between reservoir rate and power fluid rate, of about 1.

If all losses in a jet pump could be avoided, which obviously is not realistic, the performance could be like the blue line in figure 3.5. The base case loss coefficients

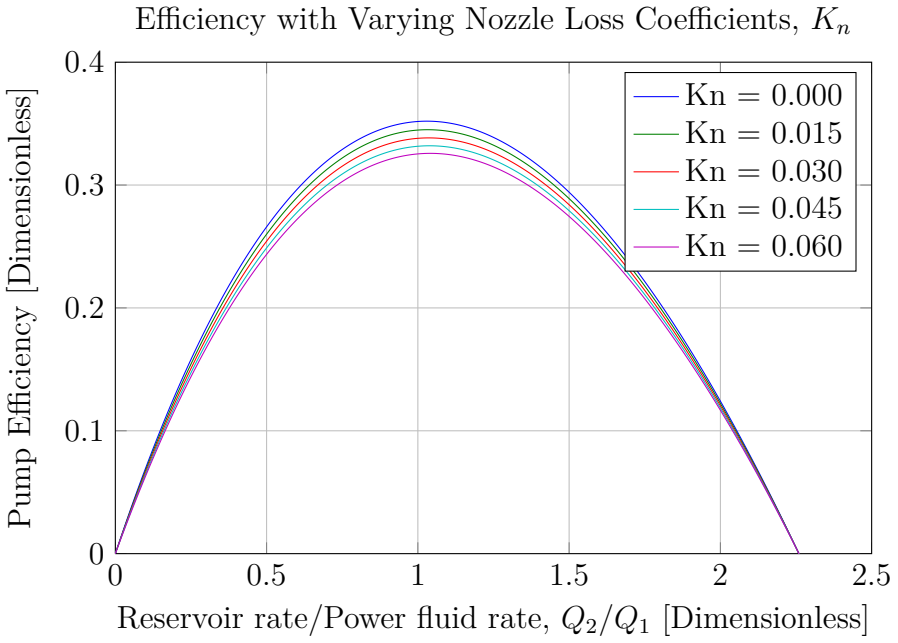

FIGURE 3.2: Efficiency with Varying Nozzle Loss Coefficients, K_n

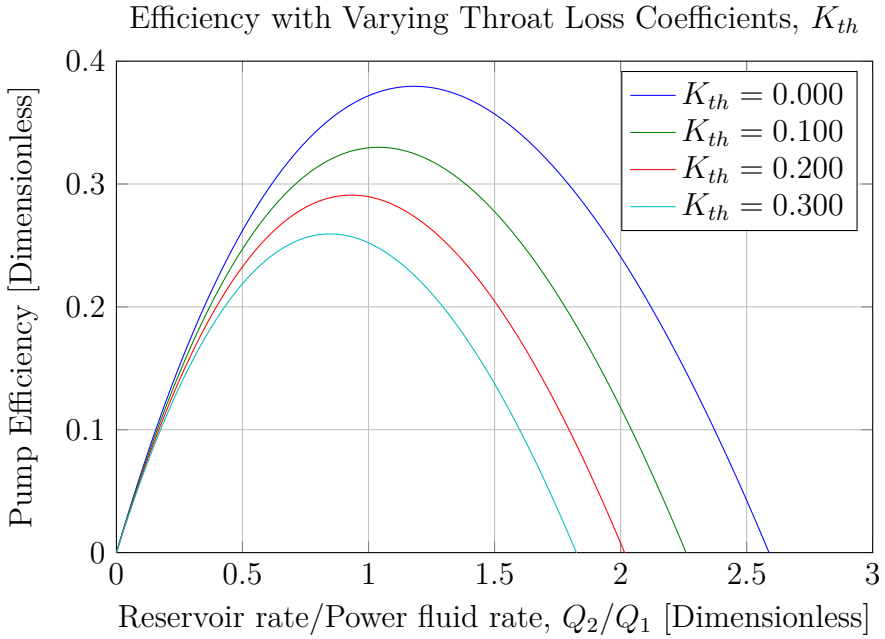

FIGURE 3.3: Efficiency with Varying Throat Loss Coefficients, K_{th}

would place the jet pump efficiency at about 0.32 for a flow-ratio of about 1. For a smooth jet pump, without loss coefficients, the efficiency is nearly 0.5 with a flow-ratio of about 1.4.

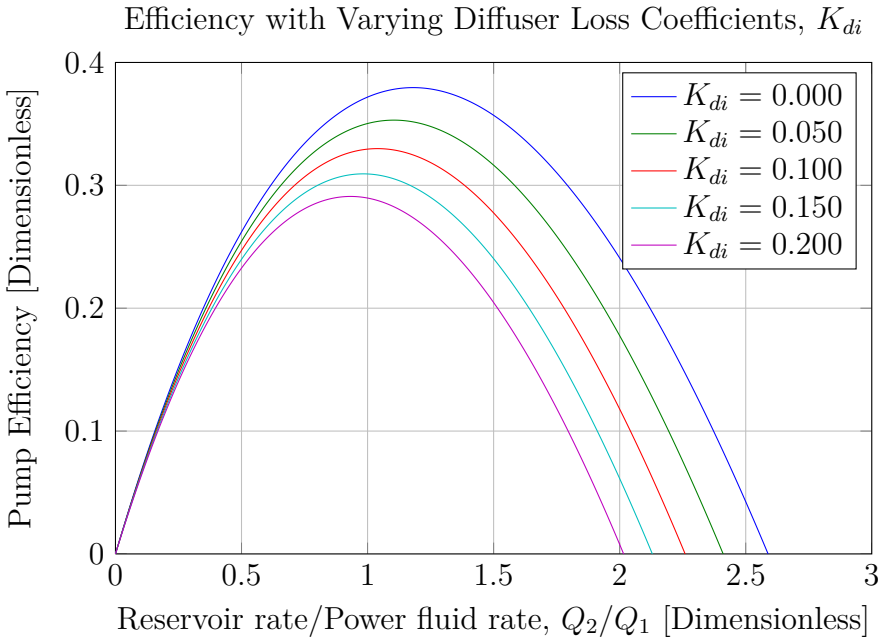

FIGURE 3.4: Efficiency with Varying Diffuser Loss Coefficients, K_{di}

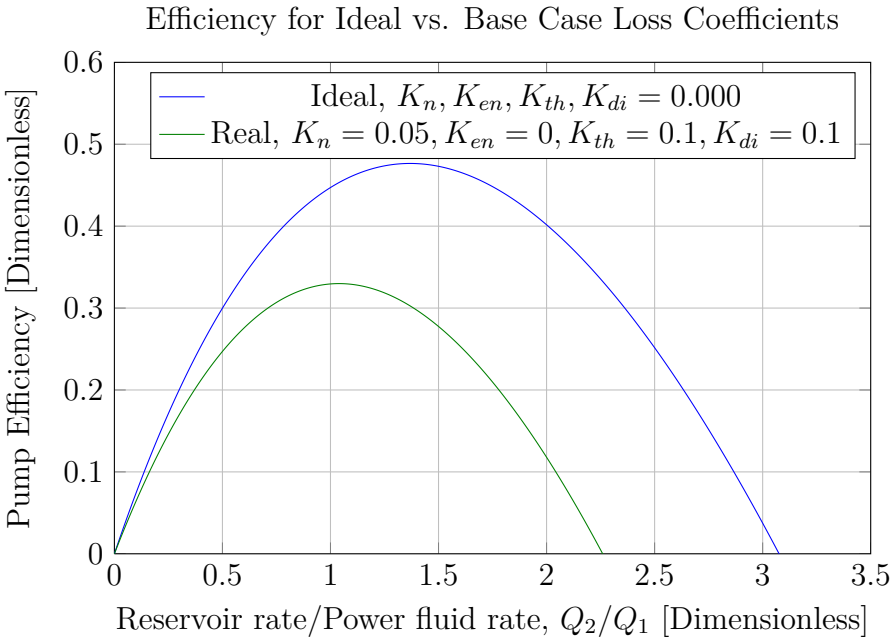

FIGURE 3.5: Pump Efficiency for Ideal and Base Case Loss Coefficients

Diffuser Angle

Cunningham[1] defines the relationship between throat and diffuser area as a, and write it as:

$$a = \frac{A_{th}}{A_{di}} \tag{3.1}$$

Figure 3.6 shows how more equal throat and diffuser areas affect pump efficiency. The pump efficiency is not affected for small ratios, but is increasing rapidly. For a throat area of 40% of diffuser area the pump efficiency has decreased by about 5%.

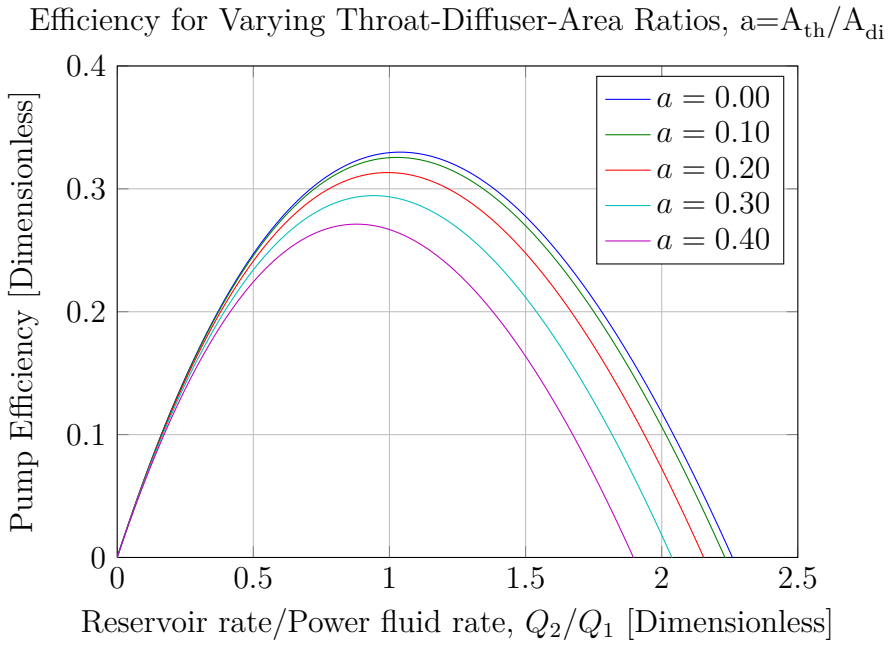

FIGURE 3.6: Efficiency with Varying Throat-diffuser-area Ratio, $a = A_{th}/A_{di}$

Power Fluid

Changing density-ratio affect the efficiency, as shown in Figure 3.7. For a decreasing reservoir density, or increasing power fluid density, the efficiency is increasing.

If water is used as power fluid a reservoir density of $800 kg/m^3$ will have a maximum efficiency of about 35% for a flow-ratio of 1.25. The figure shows that pump efficiency is decreasing as the amount of water is increasing.

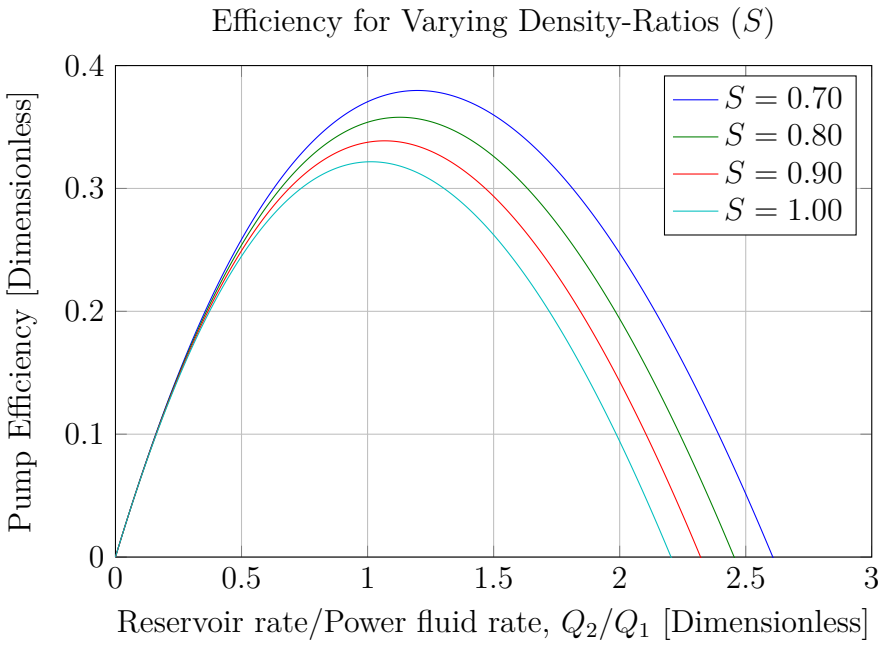

FIGURE 3.7: Efficiency for Varying Density-Ratios

The total Water-Cut must also be considered when selecting a power fluid. Figure 3.8 shows how the mixture Water-Cut increases as the reservoir Water-Cut is increasing for varying reservoir-power-fluid flow-ratios. Water is used as power fluid in this figure.

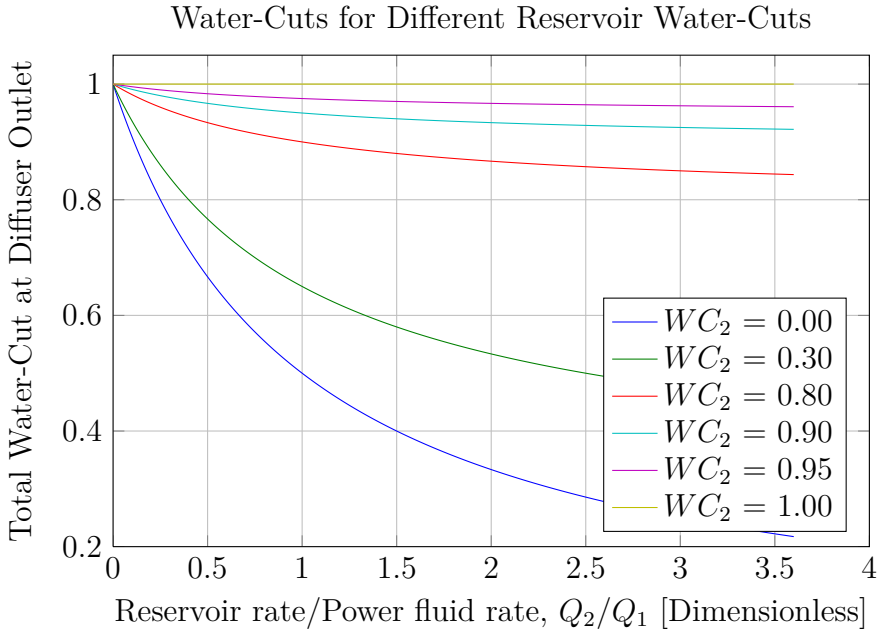

FIGURE 3.8: Diffuser Water-Cuts for Varying Reservoir Water-Cuts

3.3 Prosper Comparison

The program was connected to Prosper and necessary input parameters were acquired. The goal was to verify the performance of Prosper by comparing it with Cunningham's model. Different approaches were investigated. Figure 3.9 shows calculated rate relative to the reported rate from Prosper for varying installation depths. The figure shows that the calculated rate is half of the rate calculated in Prosper.

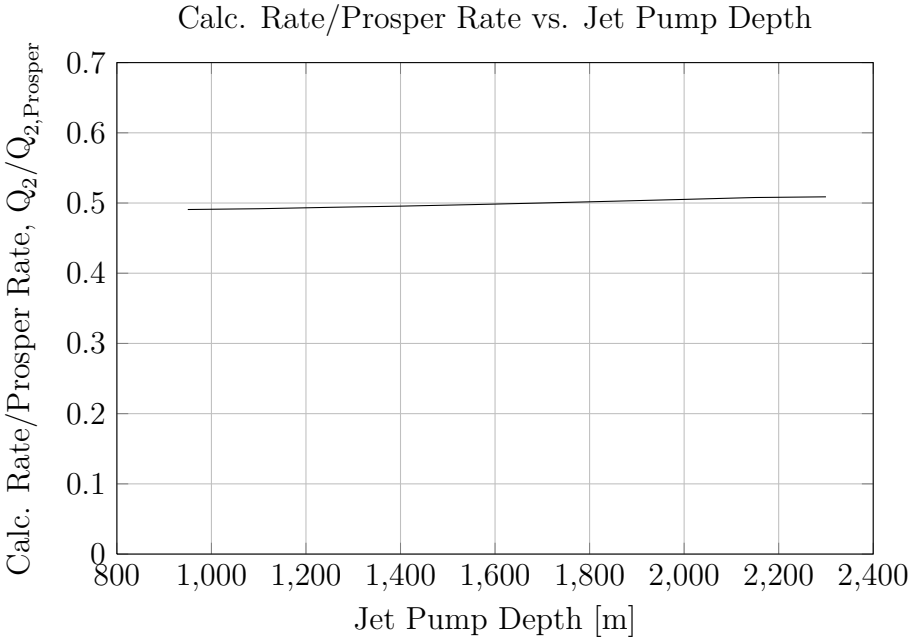

FIGURE 3.9: Calculated Reservoir Rate/Prosper Reservoir Rate for Varying Depth

Another run with varying jet pump configurations is shown in Figure 3.10. The different configurations use various nozzle- and throat-areas. This implies a range of different nozzle-throat-area ratios. The figure shows that different jet pump combinations give different deviations. The variation is from $45\% - 52\%$.

Cunningham's theory[1] is used in many publications. The developed program, based on Cunningham's model, has been verified against two independent sources. Fuch[32] and PTC[30] have comparable results for the example well and agree that Cunningham's equations are representable.

Section 2.9, about theory used in Prosper, indicate that the results should be similar[32]. This discrepancy between Prosper and Cunningham suggests that the implementation may be wrong. Since Cunningham's model is believed to

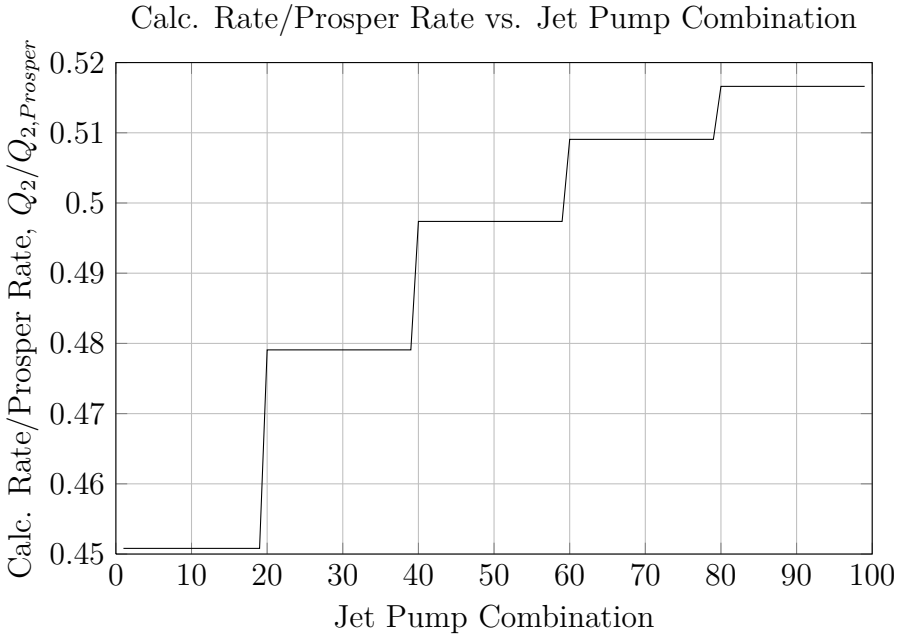

FIGURE 3.10: Calculated Reservoir Rate/Prosper Reservoir Rate for Varying Jet Pump Combinations

be correct, an implementation of this model in communication with Prosper was necessary. A self-built module calculating a jet pump installed well was developed.

3.4 Jet Pump Well Implementation

An implementation of Cunningham's jet pump in communication with Prosper was done. The method uses the same solution procedure as Prospers jet pump. A well is split in three parts as shown in Figure E.4. The solver starts by guessing a reservoir rate. The solution procedure takes the following steps:

1. *Pipe Segment 1:* Co-current calculations in Pipe Segment 1 terminating in calculated suction conditions.

2. *Power Fluid:* Calculations based on selected rate and injection pressure downhole to nozzle inlet.

3. *Jet Pump Module:* Jet pump calculations with necessary inputs. The calculated diffuser pressure from the module as output.

4. *Pipe Segment 2:* Counter-current calculations in Pipe Segment 2. The calculations are started at a known wellhead pressure. With the combined

rates, counter-current calculations are done downhole. The calculations are terminating above the jet pump, at diffuser outlet.

Two pressures are now established for the same location. Iteration on reservoir rate can be done until these pressures are approximately equal. For further details, see Appendix E.3.

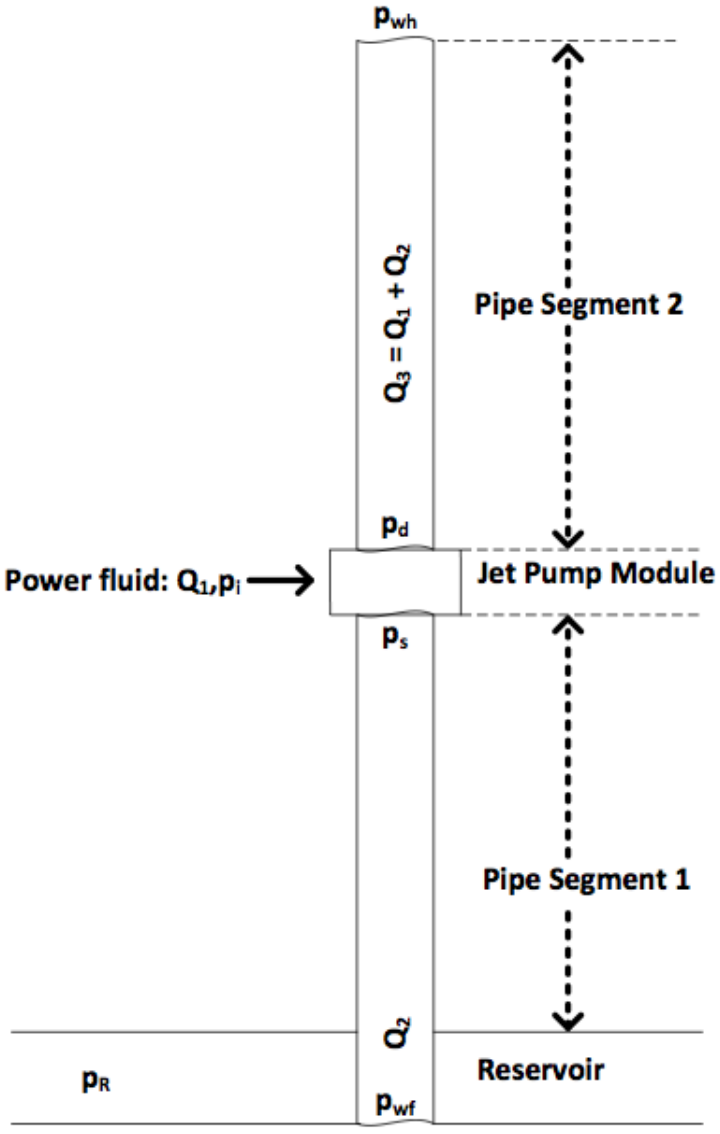

FIGURE 3.11: Implementation of Cunningham's Jet Pump

3.5 Implementation Results

Âă

A model utilizing the theory of Cunningham combined with the well hydraulic calculations from Prosper had now been established. To investigate if there were any parameters that were more determining to increased production than others a parametric study was performed. In Table 3.2 the input parameters to the model are listed. Some of these parameters were varied in a parametric study. The rest of the parameters were assumed to be constant. The goal was to study the effect on reservoir production by changing each variable at the time to see which parameters influenced production most.

Table 3.2: Well Implementation Input Parameters

Variable	**Description**	**Constraints**
$a = A_{th}/A_{di}$	Area Ratio	Dependent on throat and tubing size
D	Depth	Case dependent
K_n	Nozzle Loss Coefficient	Dependent on material selected
K_{en}	Throat Entry Loss Coefficient	Dependent on material selected
K_{th}	Throat Loss Coefficient	Dependent on material selected
K_{di}	Diffuser Loss Coefficient	Dependent on material selected
p_{wh}	Wellhead Pressure	Mainly a process related constraint
p_{pf}	Power Fluid Pressure	Available pumps at deck
Q_1	Power Fluid Rate	Available volumes for injection
$R = A_n/A_{th}$	Area Ratio	$0.15 < R < 0.35$
ρ_1	Power Fluid Density	Dependent on which fluids that are available. Could be water, oil etc.

In Figure 3.12 the characteristic performance of changing nozzle-throat-area-ratio is shown. This figure can be compared with Figure B.1. If all optimums from this figure had been plotted it would look like the plot in Figure 3.12. From all the R-curves that can be plotted, the optimum area-ratio for this specific pump is approximately $R = 0.21$. This will vary for different pumps, and is thus a beneficial parameter to optimize on.

With the initial data set, the surface injection pressure was varied. The effect is plotted in Figure 3.13. The reservoir rate obtained is increasing as power fluid injection pressure and nozzle injection pressure are increasing. However, there is a limit to the strength of casing, tubing and wellhead.

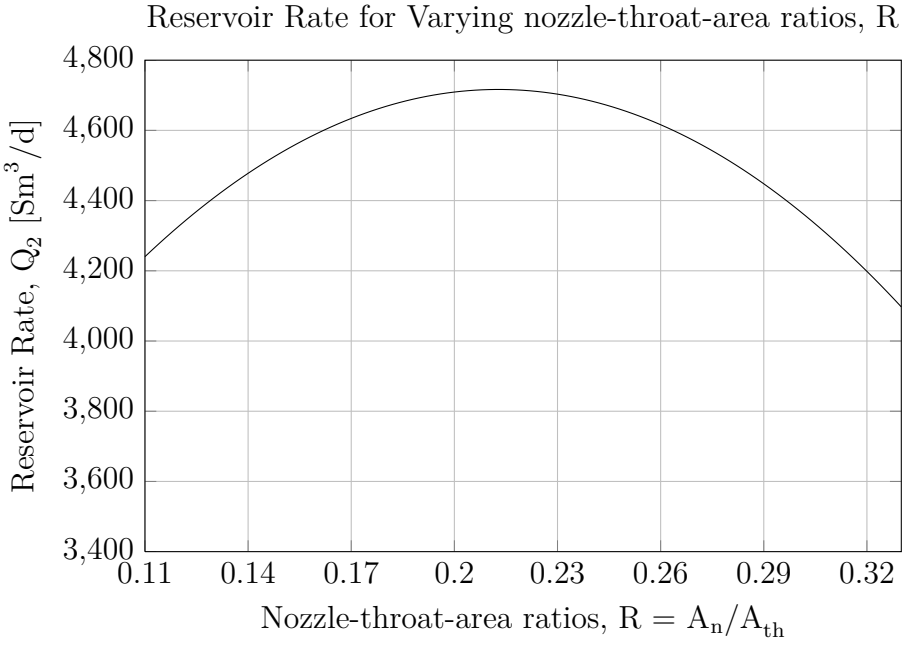

FIGURE 3.12: Reservoir Rate for Changing Nozzle-throat-area-ratios, R

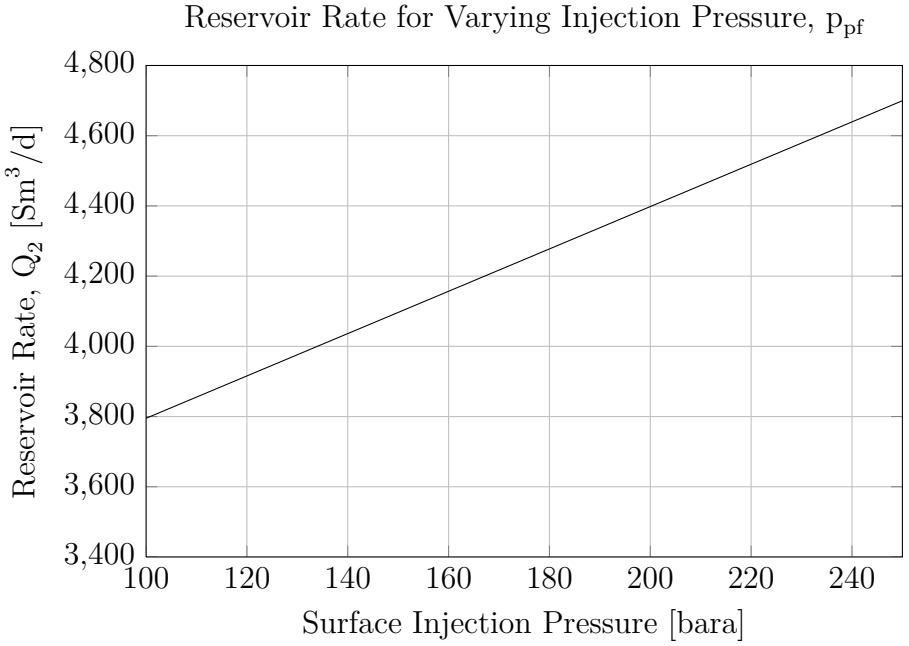

FIGURE 3.13: Reservoir Rate for Changing Surface Injection Pressure, p_{pf}

Figure 3.14 shows the benefit of increasing power fluid density within probable values. The benefit is marginal, as power fluid gets denser. The left hand part of the plot could show the performance with an oil used as power fluid. The right hand part is denser, and could be water with additives. Compared with Figure 3.13, it is evident that jet pump performance is more dependent on applied annulus wellhead pressure than denser hydrostatic column.

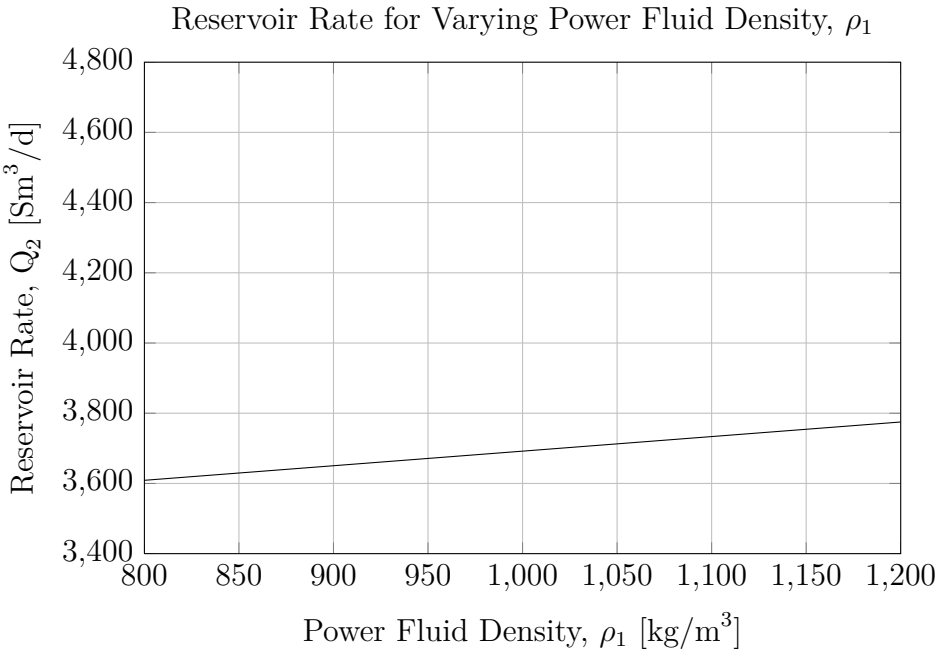

FIGURE 3.14: Reservoir Rate for Changing Power Fluid Density, ρ_1

There are three parameters that can be changed on a daily basis at the platform, and all of them are related to power fluid properties. Density and power fluid injection pressure have been presented in the two previous figures. The last parameter that can be changed is the injection rate of power fluid. Figure 3.15 displays varying reservoir rate as power fluid injection rates is increased. The green line shows well production without any artificial lift, and the blue line shows the base case jet pump. This jet pump uses the parameters listed in Table 3.3 as input.

TABLE 3.3: Base Case Parameters

Parameters	**Dimension**
$R = A_n/A_{th}$	0.23
Power fluid pressure	250 baraÂă
Power fluid density	1015 kg/m^3

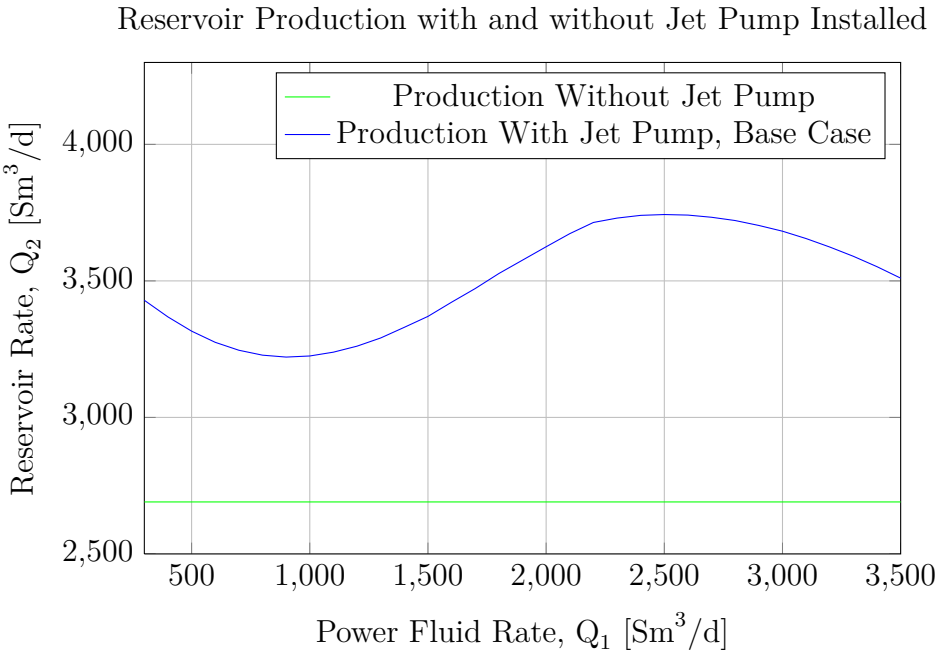

FIGURE 3.15: Reservoir Production for Well Without Jet Pump and Jet Pump Base Case

3.6 Optimization Results

Factors impacting production have been presented in the above sections. Based on these results a set of parameters was chosen for an optimization. From these sections the parameter starting points and boundaries were selected. On a daily basis the parameters that can be changed at surface are those related to power fluid. In addition, the nozzle-throat-area ratio, R, is chosen to be optimized on, due to its influence on production. Table 3.4 below shows the self-selected optimization parameters.

Table 3.4: Self-Selected Optimization Parameters

Parameters	**Dimension**
$R = A_n/A_{th}$	-
Power fluid pressure	baraÂă
Power fluid density	kg/m^3
Power fluid rate	m^3/d

To ensure that the results calculated by the optimization algorithm are physical and realistic, there are upper and lower limits defined for the algorithm. The boundaries are formulated as in Table 3.5. The optimization seeks a best fit of the four variables within the envelope given in the table.

Table 3.5: Optimization Parameter Boundaries

Lower Boundary	**Parameter**	**Upper Boundary**
0.2	$R = A_n/A_{th}$	0.3
220 $bara$	Power fluid pressure	280 $bara$Âă
$800kg/m^3$	Power fluid density	$1100kg/m^3$
$1000m^3/d$	Power fluid rate	$5000m^3/d$

Output from the optimization algorithm is the reservoir rate and the optimum combination of the four variables. The results are shown in Table 4.2.

The optimum reservoir rate found by the optimization is $3963Sm^3/d$. This specific rate is located at the top of the red curve shown in Figure 3.17. The required power fluid rate can be read from the x-axis of Figure 3.17 to be $2398Sm^3/d$. This power fluid rate is less than what the base case requires. The power fluid rate consumption for the different cases are shown in Figure 3.16.

TABLE 3.6: Optimization Results

Parameter	Value
Q_2	3963 Sm^3/d
Q_1	2398 Sm^3/d
R	0.2
p_{pf}	280 bar
ρ_1	1100 kg/m^3Âă

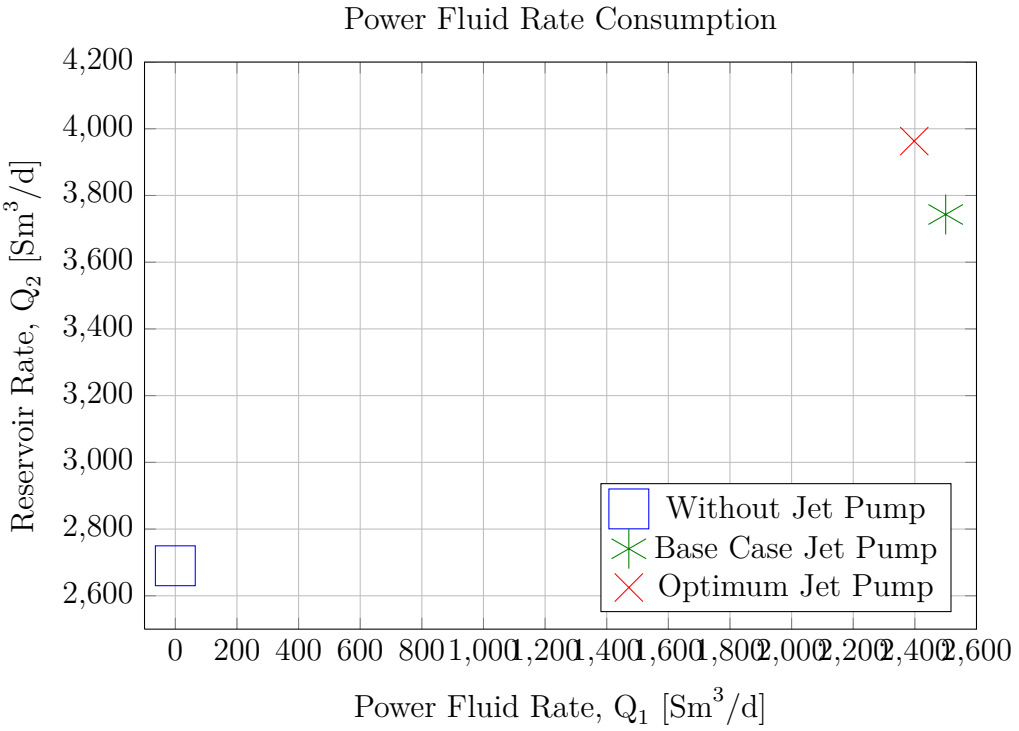

FIGURE 3.16: Power Fluid Rate Consumption

The optimum nozzle-throat-area ratio is 0.2. This value is on the lower boundary of available values. The loss coefficients used are said to be constant in the interval. This assumption makes it difficult to say which values the loss coefficients will take outside the envelope. Since loss coefficients are area-dependent an area-ratio below 0.2 could prove to increase frictional losses. The density was optimized to be $1100 kg/m^3$. The reason for this selection is the linear relationship shown in Figure 3.14. The power fluid is also selected to be the upper boundary value. The reason for this is the linear relationship of power fluid shown in Figure 3.13.

The optimized jet pump has a better performance over the values plotted in Figure 3.17. Both jet pumps have better performance than a well without any artificial lift installed.

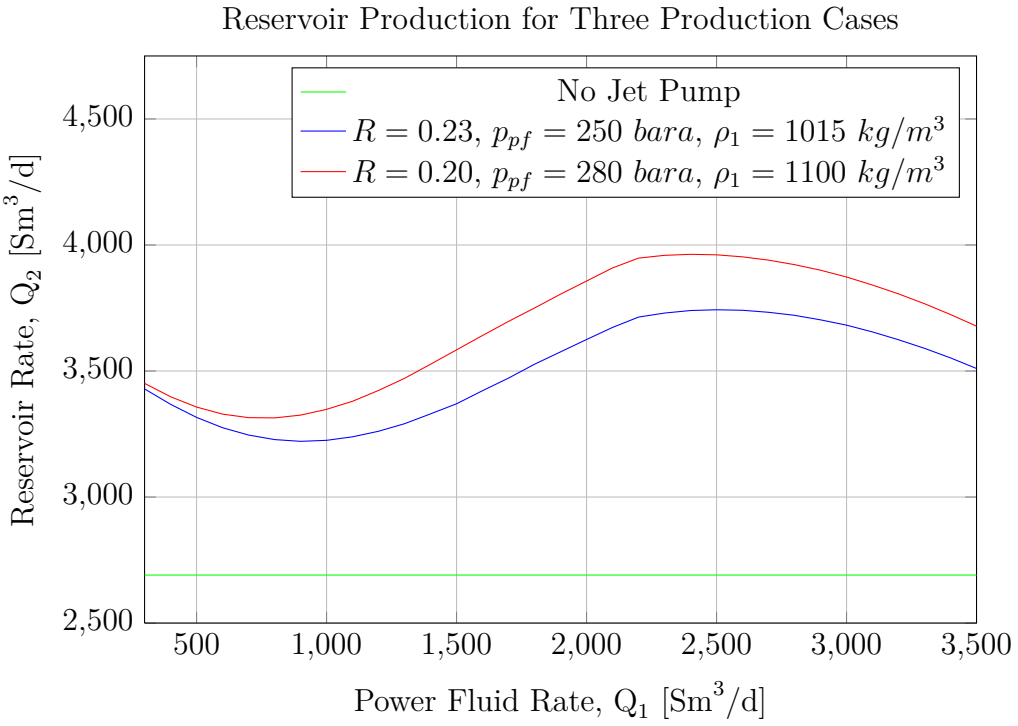

FIGURE 3.17: Reservoir Production for Well Without Jet Pump, with Jet Pump Base Case and Optimization Case

Chapter 4

Discussion

The foundation for this Master Thesis was to investigate the performance of jet pumps. Cunningham's theory[1] on jet pumps has been used in many publications and was chosen to present the energy exchange in a jet pump. The equations were programmed in Matlab and compared with the work of Fuch[32] and PTC[30]. After verifying program behaviour, the program was used to perform a sensitivity study on selected parameters.

4.1 Loss Coefficients

The loss coefficients for the different parts were varied within probable values reported in literature. In Table 2.3 the suggested loss coefficients of various authors have been listed. Loss coefficients suggested by PTC were chosen as base case values. From this base case each loss coefficient was varied in turn. The loss coefficients are reported to be dependent on area, specific pump, fluid properties, velocity and mixing related losses. The area dependence makes the loss coefficients valid for a range of nozzle-throat-area ratios. Probable R-values are between $0.2 - 0.3$, and the loss coefficients presented in Table 2.3 are based on this. The assumption of constant value loss coefficients are especially true in cases with high Reynolds Numbers[18], which can be seen in Figure 2.6. In nozzle and throat-inlet the consequence of higher loss coefficients are less, which can be seen in Figure 3.1 and 3.2. The effect of increased loss coefficients in throat and diffuser is more severe. The reason for this behaviour could be that mixing of fluids introduces mixing-related losses. Reduction in pump efficiency as the loss coefficients are

increasing can be seen in Figure 3.3 and 3.4 for throat and diffuser respectively. Additionally it is critical to obtain smooth surfaces in throat-inlet and nozzle to limit frictional losses. If the frictional losses are considerable, the jet pump lift capacity is adversely affected.

4.2 Throat-Diffuser-Area-Ratio (a)

The throat-diffuser-area-ratio (a) was changed to see what impact a smaller tubing diameter would have on jet pump performance. Increasing a means that the difference between the throat and diffuser area is less. This could be the case if the throat diameter was increasing, or the tubing ID was smaller. From Figure 3.6 there is a decreasing performance as the area-ratio is increasing. The reason for the reduced performance is the a-related term in equation A.11. This term contributes to the lowering of the diffuser pressure. A consequence of this is a reduction in pump efficiency.

Another conclusion that might be drawn from this is that jet pump installation is more favourable in a well with larger tubing. In literature it is also suggested that the diffuser angle should be gentle. An angle between $3.6° - 5.5°$ is suggested in literature. Cunningham proposes $a \approx 0$ for practical purposes in most production wells[1]. Smaller a-relationships are favourable. Smaller a could be possible if one considered a slightly longer assembly length to make the energy transition smoother. However, in practice this is hard to achieve, as the tubing inner diameter will be a constraint.

4.3 Power Fluid

The power fluid candidates are many. Both water and various types of crude has been reported as power fluid in field applications. Choice of power-fluid may vary dependency on reservoir fluid properties, fluid compatibility, location and field characteristics. For a North Sea field, water is available for injection, and both treated sea-water and formation water may be used as power fluid. Anderson et al.[33] found that applying seawater reduced efficiency. This may relate to reduced lubrication qualities, increased viscous forces and increased hydrostatic pressure downstream jet pump.

Compatibility is also important. Mixing water and formation fluids may cause undesired effects. Such effects can be permanent emulsions, which introduce demands for extra separation at the processing facilities. For a field with high Water-Cut applying water as power fluid might be a good alternative. Figure 3.8 show the mixture density at diffuser outlet as reservoir Water-Cut is increasing. As the reservoir water-cut is increasing, the total diffuser water-cut will be less affected.

From Figure 3.17 it can be seen that the optimization chose a denser power fluid. This is linked to Figure 3.7 and 3.14, where it can be seen that changing to denser power fluid improve jet pump performance. As the ratio between reservoir and power fluid increases, the efficiency is reduced. A consequence of this is that lighter reservoir fluids pumped with denser power fluid, such as water, has better efficiency than an oil power fluid jet pump case.

A jet pump is not efficient when it comes to pumping of free gas[4]. When gas is liberated from oil, as pressure is drawn down, the efficiency decreases. The fraction of gas is dependent on the bubble point of oil. If the pressure drops beneath the bubble point, gas is liberated. The efficiency decreases as free gas is introduced to the jet pump[34]. Free gas above the pump is favourable because it reduces hydrostatic pressure in the well. However, it is beneficial to place the jet pump sufficiently deep to avoid free gas in the jet pump.

4.4 Annulus

If power-fluid is transported through annulus it is also necessary to keep in mind the risk this presents to the annulus. If sea-water is used as power fluid the corrosion hazard is necessary to account for[35]. If oil is used, there is a risk of not noticing gas in annulus, due to oils capacity of holding large amounts of gas. A liberation of gas might come as a surprise when pressure is lowered. A large volume of gas in annulus is undesirable. This will not be a problem when using water, because of the low gas-water solubility. Another benefit of using denser power fluid is that the nozzle delivery pressure is increasing due to increased hydrostatic pressure. Circulation rate also affects the nozzle delivery pressure through the frictional loss. The frictional loss is proportional to velocity squared.

$$\Delta p_f = \frac{1}{2} f \rho \frac{L}{d} v^2 \tag{4.1}$$

A well is normally designed for a specific maximum pressure that it will have to withstand. The design pressure is normally based on maximum anticipated pressures to occur in the well over the field lifetime. This pressure is also the restriction for maximum injection pressure possible topside. A pressure restriction will therefore be an upper constraint for the maximum rate benefit achieved by increasing the power fluid injection pressure. Applied annulus pressure at surface will exert increased pressure in annulus, and this pressure propagates downhole to the first annuluar seal.

The pressure difference across such seals may be considerable. It is necessary to consider if the differential pressure across the seal or packer is manageable. The integrity of the seal may be compromised if the injection pressure is too high[36]. In the specialization project[37] the hazard of applying high annulus pressure was discussed. Casing burst pressure was then discussed as a probable restriction on maximum allowed annulus pressure. In addition to the two pressure restrictions mentioned, the collapse pressure of tubing might also be a restriction. Differential pressure across the tubing wall could be quite high when applying power fluid injection pressure from surface. Formation strength is also necessary to consider, as formation fracturing could cause a formation blowout. The upper boundary on injection pressure is thus dependent on several properties, and each factor has to be investigated to find the constraint.

The jet pump setting depth was discussed in the Specialization project[37]. The conclusion from this project was that it would be beneficial to place the jet pump as deep as possible. The reason for this was that the natural energy of the reservoir on its own would lift reservoir fluids to jet pump suction. Additional drawdown could be obtained through deeper setting depth. However, there are some drawbacks related to this conclusion. Figure B.3 shows the jet pump located at three different depths. The nozzle pressure is increasing as the pump is placed deeper. The benefit of increased pressure across the pump might be diminishing compared to the additional lift required above the pump. The suction pressure is also increasing as the pump is lowered for the same production rate. Increased suction pressure reduces the probability of free gas, which is beneficial because pumping free gas is not favourable. Gas dissolved in oil contributes to lower oil density, which again contributes to lower the density ratio. Lower density ratio increases efficiency (Figure 3.7). If water is used as power-fluid the hydrostatic pressure above the pump will probably increase.

4.5 Prosper Evaluation

The goal of verifying the Prosper jet pump module had to be divided into several subtasks. A specific case was calculated by Fuch[32] and PTC[30], and these calculations were assumed to be correct. The first step was thus to program Cunningham's compressible equations[1] in Matlab (Figure E.1). This model was thereafter verified against the results obtained from the sources mentioned above. Afterwards the code was converted to C#. This was done through an isolated program having the exact properties as the Matlab code. When the performance had been verified, the next step was to connect the C#-program with Prosper through OpenServer commands[38].

From Figures 3.9 and 3.10 it was concluded that the performance Prosper claimed to have was not in accordance with Cunningham's model. This was confirmed by Evensen[39]. The model used in Prosper by Brown[21] and Cunningham's model[1] were not the same. Brown's model uses total energy balance whereas Cunningham's model is based on energy conservation and momentum balance. However, the two models should give similar results[32]. This questions the implementation of jet pumps in Prosper. Instead of pursuing Prosper's jet pump module further, the self-built model based on Cunningham's equations was developed.

The next step was thus to build a model that had a familiar basis, establishing trustworthy results. The thought behind this model was that a well would converge for a correct reservoir rate. At the balance point there would be sufficient energy to lift the combined fluids to the processing facilities. The convergence criteria was chosen so that counter-current pressure calculated from wellhead downhole should be approximately equal to the diffuser pressure calculated by the jet pump module. This idea is summarized in Figures E.3 and E.4.

4.6 Simulation Results

A sensitivity was performed based on the input parameters to the algorithm presented in Table 3.2. The plots are presented in Figure 3.12, 3.13, 3.14 and 3.15. From these figures it might be concluded that there are some factors that are affecting performance more than others. A visual proof of how the surface pump affects jet pump performance can also be seen in Figure B.4.

Figure 3.12 shows the maximum production possible for different nozzle-throat-area ratios. This factor will change for different pumps, and for different inputs. The optimum moves as jet pump properties are changed. The flow-ratio of reservoir flow to power fluid flow is also changing location.

In Figure 3.13 the power fluid injection pressure is changed. This has earlier been discussed as being dependent on well design pressure. The linear relationship favours applying as high an injection pressure as possible. For a field application the cost of pumping power fluid must be considered. In this Master Thesis injection rate and pressure have been treated as independent properties. For a real pump these properties are connected through the pump curve, which relate rate to available pressure.

There also exist a linear relationship for the power fluid density. Figure 3.14 shows that increasing power fluid density increases reservoir production. The increase is less than the increase obtained through higher injection pressures. As for the injection pressure, the density can be weighted against the cost of pumping denser fluid. The compatibility and dynamic issues mentioned in SectionÂă4.3 must also be recalled in the decision process. If additives are necessary to obtain higher densities it should be considered if such additives might introduce friction and errosion in the jet pump.

4.7 Optimization

Four parameters where chosen to be optimized on based on Section 3.5. The IPOPT optimization algorithm was utilized and the optimization was tuned to work properly. A first guess of the four optimization parameters was selected to be the base case. Boundaries were defined, and the optimization was begun. The program was time-consuming but required modest computer power. The optimum combination within the specific range is shown in Table 4.1.

These results confirm the anticipated results based on Figure 3.12, 3.13 and 3.15. As discussed in Section 2.10 there are several parameters mentioned in literature as possible optimization candidates. The optimization parameters are those that are possible to change in the short term. The parameters in Table 2.4 are possible to include at a later stage. Optimization on these parameters could indicate a the jet pump that would be the overall best over the predicted well changes. Change

Table 4.1: Optimum Combination of Selected Variables

Parameter	**Value**
Q_2	3963 Sm^3/d
Q_1	2398 Sm^3/d
R	0.2
p_{pf}	280 bar
ρ_1	1100 kg/m^3Âă

in productivity, reservoir pressure, water-cut, etc. could be optimized on to find an appropriate pump for the reservoir predicition.

In Figure 3.17 the optimized jet pump is evaluated over a range of power fluid rates and can be seen to be the overall best alternative over the selected range. From this figure the optimum performance for the different alternatives can be seen.

Table 4.2: Comparison Of the Optimas for Each Alternative

Configuration	**Rate**	**Percent Improvement**
Without Jet Pump	2690.46 Sm^3/d	-
Base Case Jet Pump	3743 Sm^3/d	39%
Optimized Jet Pump	3963 Sm^3/d	47%

Additionally, the power fluid requirements are less for the optimized solution. This is evident since the optimum in Figure 3.17 is shifted leftwards for the optimum solution. This can also be seen on the power fluid rate consumption in Figure 3.16. A well without jet pump is naturally demanding no power fluid. Reservoir rate from the two jet pumps are higher. However, the optimum combination also demands less power fluid and produces more than the base case.

The benefit of optimizing on power is not stressed in Figure 3.16. The injection rate starting point had already been indicated by Figure 3.15. If this information had not been known, the starting point in Figure 3.16 could be located much further away from the optimum injection rate.

4.8 Model Evaluation, Source of Errors and Future Work

Model Evaluation

The model developed somewhat difficult to understand for a first time viewer. The program contains close to 1000 lines and navigation is challenging. It is believed that this model is better due to the theoretical framework the model is built on. Cunningham's model[1] is used by many publications within the industry. Consequently, a model built on this is believed to be trustworthy.

The challenge for a user is the understanding of a jet pump, and how the different parameters might affect its performance. When design parameters, such as loss coefficients and geometrical ratios, are defined there are basically only the parameters mentioned in Table 3.4 that need to be changed by the user.

The program is run in Visual Studio, and it is therefore necessary to have Visual Studio and Prosper installed to run the model. A future project could include building an executable file that could be run from any computer having only Prosper installed.

In this model the frictional losses in annulus are not accounted for. The implication of this is that the nozzle injection pressure probably is a bit too high. However, for reasonable injection rates and sufficient annulus area, this is probably small compared to the hydrostatic delivery pressure. To run this model it is also necessary to assume the following;

- Which power fluid rate and pressure is available.
- Range of power fluid densities available.
- Jet pump specifications such as loss coefficients and range of possible nozzle combinations.
- Depths.

A disadvantage of this model is that it assumes constant jet pump location depth. From Figure B.3 it would be interesting to see how changing depths affect performance. Prosper divides a well into 16 nodes. This makes it somewhat difficult to

change to desired jet pump location without modifying nodes. The jet pump is placed at such nodes. As the selected node is changed, the gradient table lengths used to calculate necessary input to the algorithm are also changed. This complicates the calculations somewhat. This shortcoming could be solved, but was not prioritized.

Sources of Errors and Uncertainties

- The model is built the theoretical work of others. Small misprints may have been included unintentionally. Errors done as the code was programmed in Matlab is also a possibility.
- Annular frictional losses are not accounted for, giving a optimistic nozzle delivery pressure. These frictional losses could be accounted for with known annular area.
- One-dimensional theory developed for jet pumps may give wrong impression on performance. By verifying performance against real pumps this could be confirmed or disconfirmed.
- Frictional losses mentioned are based on theoretical suggestions. Constant loss coefficient are questionable.
- The Inflow Performance Relationship (IPR) used is a simple expression. Prosper has a inflow analysis package, and this could be included to calculate relastic reservoir rates. This could contribute to increased runtimes. Including such relationship could be weighted against the uncertainty added by not doing it.

Future Work

There are still a number of things that needs to be assessed before reaching the final goal of introducing jet pumps as an equal artificial lift alternative to Gas Lift and Electrical Submersible Pumps. The selection procedure, both for engineers and in Prosper, is somewhat complicated. Enabling people to select jet pumps as the artificial lift alternative will involve the following steps:

1. Make a tutorial for jet pump calculations.

2. Have a program that utilize the same basis as the ESP selection in Prosper. This program should be executable from all computers that have Prosper installed such that the threshold is as low as possible. Output from the program could be a prioritized list of jet pumps suitable for the specific well.

3. Incorporate optimization routine for Gas Lift, Jet Pump and Electrical Submersible Pumps in such a way that one program could take the specified well and find the optimum artificial lift alternative for the user-specified restrictions.

Conclusion

In this Master Thesis jet pumps have been reviewed. The factors impacting jet pump performance have been investigated through a verified model. The performance of Prosper has been compared to Cunningham's model. A self-built model has been developed to calculate a jet pump installed well. An optimization has been performed on selected values to find the optimum combination of these. Based on the discussion in Chapter 4, the following conclusions can be done.

- Jet pump performance and efficiency is dependent on several factors, such as: loss coefficients, densities, geometrical configurations, depth location, injection rate and pressure. For the example well the optimum efficiency is 0.32.
- Cunningham's model was programmed both in Matlab and C# and a comparison with Prosper's model was performed. The results showed a discrepancy that was believed to be implementation related. Cunningham and Brown (Prosper's theoretical framework) should give fairly similar results.
- A self-built model was implemented to calculate a jet pump installed well. Some parameters were varied to investigate changes in production. Based on these results a optimization was suggested.
- An optimization was performed and the results showed considerably higher rates achieved compared to a well without jet pump installed. The increase was 39% and 47% for the two jet pumps, base case and optimized pump respectively, compared to a well without artificial lift installed.

Bibliography

[1] Karassik I.J., Messina J.P., Cooper P., and Heald C.C. *Pump Handbook*. New York: McGraw-Hill; 2007, 3 edition.

[2] Dollar F.O. SPE21117-MS - Drill Stem Testing with Jet Pump. In *SPE Latin America Petroleum Engineering Conference, 1990*, pages 4. DOI: 10.2118/21117–MS.

[3] Allan J.C., Moore P.C., and BP Exploration Ltd. SPE19279 - Design and Application of an Integral Jet Pump/Safety Valve in a North Sea Oilfield. *SPE, 1989*, pages 18. DOI:10.2118/19279–MS.

[4] Grupping A.W., Coppes J.L.R, and Groot J.G. SPE15670 - Fundamentals of Oilwell Jet Pumping. *SPE Production Engineering, 1988*, 3(1):9–14. DOI:10–2118/15670–PA.

[5] Benson T. Mach Number [Internet]. [cited 2013 march 04]. available at: http://www.grc.nasa.gov/www/k-12/airplane/mach.html.

[6] Winoto S.H., Li H., and Shah D.A. Efficiency of Jet Pumps. *Journal of Hydraulic Engineering, 2000*, 126(2):150–156. DOI: 10.1061/(ASCE)0733–9429(2000)126:2(150).

[7] Wærp N.P. Jet Pump. [Masters Thesis], Norwegian University of Science and Technology, Trondheim, 2010.

[8] El Sawaf I.A., Halawa M.A, Younes M.A., and Teaima I.R. Study of the Different Parameters that Influence on the Performance of Water Jet Pump. *Fifteenth International Water Technology Conference, IWTC*, 2011.

[9] Prabkeao C. and Aoki K. Study on the Optimum Mixing Throat Length for Drive Nozzle Position of the Central Jet Pump. *Journal of Visualization*, 2005. 8(4):347–355.

[10] Cunningham R.G. and Dopkin R.J. Jet Breakup and Mixing Throat Lengths for the Liquid Jet Gas Pump. *J. Fluid Engineering, Trans. ASME, 1974*, 93(3):216–226. DOI: 10.1115/1.3447144.

[11] Lea J.F., Nickens H.V., and Wells M. *Gas Well Deliquification*. Gulf Professional Publishing, 2 edition, 2011.

[12] Bonnington S.T. and King A.L. *Jet Pumps and Ejectors: A State of the Art Review and Bibliography*. BHRA Fluid Engineering, 1976.

[13] Cunningham R.G. and Hansen R.G. Jet Pump Cavitation. *Trans. ASME Journal of Basic Engineering, 1970*, 92(3):483–494. DOI: 10.1115/1.3425040.

[14] Fuch P.H. Jet Pump Design [Internal Statoil Documents]. 2013 (Unpublished).

[15] Teamia I.R., Younes M.A., El Sawaf I.A., and Halawa M.A. Experimental Study of the Effect of Mixing Chamber Length and Diffuser Angle on the Performance of Dredging Jet Pump. In *Sixteenth International Water Technology Conference*, number 16, 2012.

[16] Kumar A., Telang M.K, and De S.K. SPE53912-MS - Innovative Techniques to Maintain Production from Problematic Indian Offshore Field - a Case History. In *Latin American and Caribbean Petroleum Engineering Conference, 1998*, pages 11. DOI:10.2118/53912–MS.

[17] Riva M., De Ghetto G., and Paolo G. SPE27595 - Jet Pump Testing in Italian Heavy Oils. In *European Production Operations Conference and Exhibition, 1994*, pages 12. DOI:10.2118/27595–MS.

[18] Hatziavramidis D. SPE19713 - Modeling and Design of Jet Pumps. *SPE, 1991*, 6(4):413–419. DOI: 10.2118/19713–PA.

[19] Mikhail S. and Abdou H.A.M. Two-phase Flow in Jet Pumps for Different Liquids. *Journal of Fluids Engineering, 2005*, 127(5):1038–1042. DOI: 10.1115/1.1990203.

[20] Petroleum Experts. IPM [Internett]. [cited 2013 feb]. available at: http://www.petex.com/includes/download.php?id=1.

[21] Brown K.E. *The Technology of Artificial Lift Methods*, volume 2b. University of Wisconsin - Madison. PPC Books, 1980.

[22] Heylighen F., Cliff J., Turchin V., and Bollen J. Optimization [Internet]. [cited 2013 may 13]. available at: http://pespmc1.vub.ac.be/asc/optimizatio.html.

[23] Wächter A. and Vigerske L.T. On the Implementation of a Primal-Dual Interior Point Filter Line Search Algorithm for Large-Scale Nonlinear Programming. *Mathematical Programming, 2006*, 106(1):25–57. DOI: 10.1007/s10107–004–0559–y.

[24] Gill P.E. and Leonard M.W. Limited-memory Reduced-Hessian Methods for Large-scale Unconstrained Optimization. *Society of Industrial and Applied Mathematics, 2003*, 14(2):380–401. DOI: 10.1137/S1052623497319973.

[25] Andreussi P., Ansiati A., Faluomi S., Senna S., Sodini S., Dellarole E., and Battaia C. SPE90369 - Application of MJPs in Oil&Gas Fields. In *SPE Annual Technical Conference and Exhibition, 2004*, pages 5. DOI: 10.2118/90369–MS.

[26] Corteville J.C., Ferschneider G., Hoffman F.C., and Valentin E.P. SPE16923-MS - Research on Jet Pumps for Single and Multiphase Pumping of Crudes. In *SPE Annual Technical Conference and Exhibition, 1987*, pages 12. DOI: 10.2118/16923–MS.

[27] B. Jiao, Blais R.N., and Schmidt Z. SPE18190-PA - Efficiency and Pressure Recovery in Hydraulic Jet Pumping of Two-Phase Gas/Liquid Mixtures. *SPE Production Engineering, 1990*, 5(4):361–364. DOI: 10.2118/18190–PA.

[28] De Ghetto G. and Giunta P. SPE27595-MS - Jet Pump Testing in Italian Heavy Oils. *SPE, 1994*, (12. DOI: 10.2118/27595-MS).

[29] Chavan C., Jha M., Singh M.K., and Singh R. SPE163116-MS - Selection and Successful Application of Jet Pumps in Mangala Oil Field: A Case Study. In *SPE Artificial Lift Conference and Exhibition, 2012*, pages 24. DOI: 10.2118/163116–MS.

[30] Allan J.C. Jet Pump Seminar. Presented on Jet Pump Seminar;. December 2012; Rotvoll.

[31] AutoDiff. [Internet]. [cited 2013 may 21]. available from http://autodiff.codeplex.com/.

[32] Fuch P.H. Kommentar til mail med presentasjon. [Internal Statoil Documents]. 2013 (Unpublished).

[33] Anderson J., Freeman R., and Pugh T. SPE94263 - Hydraulic Jet Pumps Prove Ideally Suited for Remote Canadian Oil Field. In *SPE Production Operations Symposium, 2005*, pages 6. DOI: 10.2118/94263–MS.

[34] Artificial Lift Methods Overall Comparison [Internet] [cited may 30] Available from: http://engineering.com.

[35] Johnsen R. Introduction to Material Selection. [Unpublished Lecture Note]. TPG4200: Subsea Production Systems, lecture given; February 2011.

[36] Asheim H. Master Thesis Meeting. Meeting, June 2013.

[37] Liknes F. Jet Pumps. [specialization Project], Norwegian University of Science and Technology, Trondheim, 2012.

[38] OpenServer. [Internet]. [cited 2013 apr]. Available from: http://www.petex.com/products/?ssi=7.

[39] Evensen E. Artificial Lift - Jet Pump, [Internal Statoil Documents on Prosper]. 2013 (Unpublished).

[40] Peirce J.W., Burd J.A., Schwartz G.L., and Pugh T.S. SPE114912 - Formation Powered Jet Pumps Used at Kuparuk Field in Alaska, Denver Colorado. *SPE, 2008*, pages 14. DOI 10.2118/114912–MS.

[41] Standards Norway. *Well Integrity in Drilling and Well Operations. NORSOK :Standards Norway; 2004 August. Report No: D-010.*

[42] Schlumberger Oilfield Glossary. [Internet]. [cited 2012 nov]. Available from: http://www.glossary.oilfield.slb.com/.

[43] Weatherford. Hydraulic Jet Pump [Internet]. [cited 2012 nov]. available at: http://www.weatherford.com/weatherford/ groups/web/documents/weatherfordcorp/wft007479.pdf.

[44] Clegg J.D., Bucaram S.M., and Heln Jr. N.W. SPE24834 - Reccomendations and Comparisons for Selecting Artificial-lift Methods. *JPT Distinguished Author Series, 1993*, 45(12):1128–1131, 1163–1167. DOI: 10.2118/24834–PA.

[45] MathWorks. Solve system of nonlinear equations - MATLAB fsolve [Internet]. [cited 2013 may 15]. available at: http://www.mathworks.se/help/optim/ug/fsolve.html.

[46] Note on Alglib Package [Internet]. [cited april 2013 29]. available at: www.alglib.net.

[47] E.W. Weisstein. Jacobian: From MathWorld - A Wolfram Web Resource [Internet]. [cited 2012 apr 30]. available at: www.mathworld.wolfram.com/jacobian.html.

List of Figures

List of Tables

Abbreviations

ALRDC	**A**rtificial **L**ift **R&D** **C**ouncil
AD	**A**utomatic **D**ifferentiationÂă
API	**A**merican **P**etroleum **I**nstitute
ASCSSV	**A**nnular **S**urface **C**ontrolled **S**ub-Surface **S**afety **V**alve
BHP	**B**ottom **H**ole **P**ressure
DHSV	**D**ownhole **S**afety **V**alve
ESP	**E**lectrical **S**ubmersible **P**ump
FPJP	**F**ormation **P**owered **J**et **P**umps
GOR	**G**as-**O**il-**R**atio
GUI	**G**raphical **U**ser **I**nterface
GVF	**G**as **V**olume **F**actor
IPR	**I**nflow **P**erformance **R**elationship
NORSOK	**N**orwegian Continental Shelf Safety Regulation
PI	**P**roductivity **I**ndex
Re	**R**eynolds **N**umberÂă
SCSSV	**S**urface **C**ontrolled **S**ub-Surface **S**afety **V**alve

Physical Constants

Gravity	g	=	$9.81\ {}^{m}/_{s^2}$
Gas Constant	R	=	$8.3144621(75)\ {}^{J}/_{molK}$

Symbols

di	diffuser	-
en	throat-entry	-
i	power fluid inlet	-
n	nozzle	-
s	suction	-
o	throat inlet	-
td	throat + diffuser	-
th	throat outlet	-
1	primary flow (power flow)	-
2	secondary flow (reservoir flow)	-
3	mixture flow (power + reservoir)	-
a	A_{th}/A_d	-
A	area	m^2
B	formation volume factor	$^{m^3}/_{Sm^3}$
c	$(1-R)/R$	-
K	loss coefficient	-
L	nozzle-throat spacing	-
L_{th}	throat length	m
M	volumetric flow-ratio (Q_2/Q_1)	-
Ma	mach-number	-
p	pressure	bara

p_v	vapor pressure	bara
P	Power	W
q	standard rate	$^{Sm^3}/_{s}$
Q	actual rate	$^{m^3}/_{s}$
R	A_n/A_{th}	-
R_{so}	solution gas-oil-ratio	$^{Sm^3}/_{Sm^3}$
S	density ratio ρ_2/ρ_1	-
T	temperature	K
v	velocity	$^{m}/_{s}$
Z	jet dynamic pressure	bara
η	efficiency	-
γ	gas/primary liquid density ratio (ρ_G/ρ_1)	-
ϕ	gas/primary volumetric flow ratio (Q_g/Q_1)	-
ρ	density	$^{kg}/_{m^3}$
σ	cavitation coefficient	-

Appendix A

Cunningham's Jet Pump Equations

The flow in each part is described in Section 2.1. In this chapter all the equations are expressed explicitly. These equations were programmed in Matlab to calculate jet pump performance. The first section list the compressible equations that were used in the program. The second section describe the incompressible equations.

The incompressible equations are believed to be valid for cases with high water-cuts, or diminishing amounts of gas[1]. The compressible equations, on the other hand, take expansion and contraction of gas into account.

The brief description given below for each part in the subsequent section is mainly valid for the incompressible equations. The description is therefore omitted in the second section.

A.1 Compressible Equations

A.1.1 Nozzle Equation

Power fluid enter the jet pump through the nozzle and discharge in throat as a high velocity jet. The energy translation is expressed using Bernoulli's equation.

$$p_i + \tfrac{1}{2}\rho_1 v_i^2 = p_o + \tfrac{1}{2}\rho_1 v_n^2 + K_n \tfrac{1}{2}\rho_1 v_n^2 \tag{A.1}$$

Which may be rewritten as

$$p_i - p_o = Z(1 + K_n) \tag{A.2}$$

Where the nozzle discharge pressure, p_o, is approximately equal to the suction pressure, p_s. This approximation is valid since the nozzle usually is retracted from throat. The jet is thus discharging against a pressure that is closer to the suction pressure. Z is the jet dynamic pressure defined as

$$Z = \tfrac{1}{2}\rho_1 v_n^2 \tag{A.3}$$

A.1.2 Throat-entry Equation

The reservoir fluid may contain gas. It is thus necessary to account for the changing volumes of gas as the reservoir fluid flow through the pump. The volume of gas entering the pump is assumed to be known. To calculate the volume of gas in the other jet pump parts the ideal gas law applied. The ideal gas law is assumed to be applicable and is formulated as.

$$pV = NRT \tag{A.4}$$

By using this definition, the relative difference of pressure and volume at two locations can be expressed as.

$$pQ_G = p_s Q_{Gs} \tag{A.5}$$

Now, recalling the definition of ϕ from Abbreviations, relating gas rate to power fluid injection rate, the amount of gas at any location in the jet pump can be calculated by

$$\phi_i = \phi_s \frac{p_s}{p_i} \tag{A.6}$$

Utilizing this and assuming isothermal behaviour the pressure change from suction to throat inlet can be formulated from Bernoulli's equation, and is expressed by equation A.7.

$$M(p_s - p_o) + p_s \phi_s ln(\tfrac{p_s}{p_o}) = Z\frac{SM + \gamma\phi_s}{c^2}(1 + K_{en})(M + \phi_s \frac{p_s}{p_o})^2 \tag{A.7}$$

A.1.3 Mixing-throat Momentum Equation

The fluids are mixed in throat. The momentum equation says that momentum of fluids leaving the control volume, minus momentum of fluids entering, equals the external force; that is, the pressure change across the control volume surface ($A_{th} = A_n + A_e$)[4]. Combining this with the established volume relationship for gas, the balance can be written as

$$A_{th}(p_o - p_t) - \int dFr = (m_1 + m_2 + m_G)V_{3t} - m_1 v_n - (m_2 + m_G)V_{2Go} \tag{A.8}$$

Which in its final and condensed form can be expressed as

$$(p_o - p_t) = ZR^2(2 + K_{th})(1 + SM + \gamma\phi_s)(1 + M + \phi_s\frac{p_s}{p_t}) \\ - 2ZR - 2Z\frac{R^2}{1-R}(SM + \gamma\phi_s)(M + \phi_s\frac{p_s}{p_o}) \quad \text{(A.9)}$$

A.1.4 Diffuser Equation

In diffuser the kinetic energy of the commingled fluids are converted to potential energy. This pressure increase in diffuser is described in a similar way as in throat-inlet and nozzle. The energy change is described by the continuity equation. The equation describing the flow from throat to diffuser outlet is described by the integral

$$\int_t^d \frac{dP}{\rho} + \int_t^d VdV + \int_t^d \frac{\Delta P_f}{\rho_{3t}} = 0 \quad \text{(A.10)}$$

which in its final form can be expressed by

$$(p_d - p_t) + \frac{p_s\phi_s}{(1+M)}ln(\frac{p_d}{p_t}) = ZR^2\Big\{\frac{1 + SM + \gamma\phi_s}{(1+M)}\Big\}\times \\ \Big((1 + M + \phi_s\frac{p_s}{p_t})^2 - a^2(1 + M + \phi_s\frac{p_s}{p_d})^2 - K_{di}(1 + M + \phi_s\frac{p_s}{p_t})(1+M)\Big) \quad \text{(A.11)}$$

A.2 Incompressible Equations

Incompressible Nozzle Equation

$$P_i + \tfrac{1}{2}\rho_1 v_i^2 = P_o + \tfrac{1}{2}\rho_1 v_n^2 + K_n\tfrac{1}{2}\rho_1 v_n^2 \quad \text{(A.12)}$$

This may be rewritten as

$$P_i - P_o = Z(1 + K_n) \tag{A.13}$$

Where

$$Z = \tfrac{1}{2}\rho_1 v_n^2 \tag{A.14}$$

Incompressible Throat-entry Equation

$$M(p_s - p_o) = Z(1 + K_{en})\frac{SM^2}{c^2} \tag{A.15}$$

Incompressible Throat Equation

$$p_t - p_o = Z\Big[2R + SM^2\frac{R^2}{1-R} - R^2(2 + K_{th})(1 + SM)(1 + M)\Big] \tag{A.16}$$

Incompressible Diffuser Equation

$$p_d - p_t = ZR^2(1 + SM)(1 + M)(1 - K_{di} - a^2) \tag{A.17}$$

Appendix B

Incompressible Jet Pump Program and Sensitivity

B.1 Incompressible Program

The Matlab program developed for the incompressible equations are attached in Appendix F.1.1. The incompressible equations presented in Appendix A.2 can now be solved sequentially starting by calculating the jet dynamic pressure. The jet dynamic pressure is the force imparted on the reservoir flow in throat, due to pressure difference between suction and nozzle injection pressure. The pressures through the pump are then found sequentially. The program terminates after the dimensionless pressure ratio (N) and efficiency has been calculated. Dimensionless head recovery is defined as

$$N = \frac{p_d - p_s}{p_i - p_d} = \frac{\Delta p_{reservoir\ \ fluid}}{\Delta p_{power\ \ fluid}} \tag{B.1}$$

With pressure ratio defined, the pump efficiency can be defined as

$$\eta = \frac{Q_2}{Q_1}\frac{p_d - p_s}{p_i - p_d} = MN \tag{B.2}$$

By plotting the efficiency and pressure-ratio as a function of flow-ratio we are able to decide on which jet-pump area ratio that have the best overall efficiency for the range of flow-ratios. The jet-pump area ratio is defined as:

$$R = \frac{A_n}{A_{th}} \tag{B.3}$$

Figure B.1 can be understood as increasing reservoir flow causes higher mixing-related losses. The result from those losses are less pressure increase across the pump.

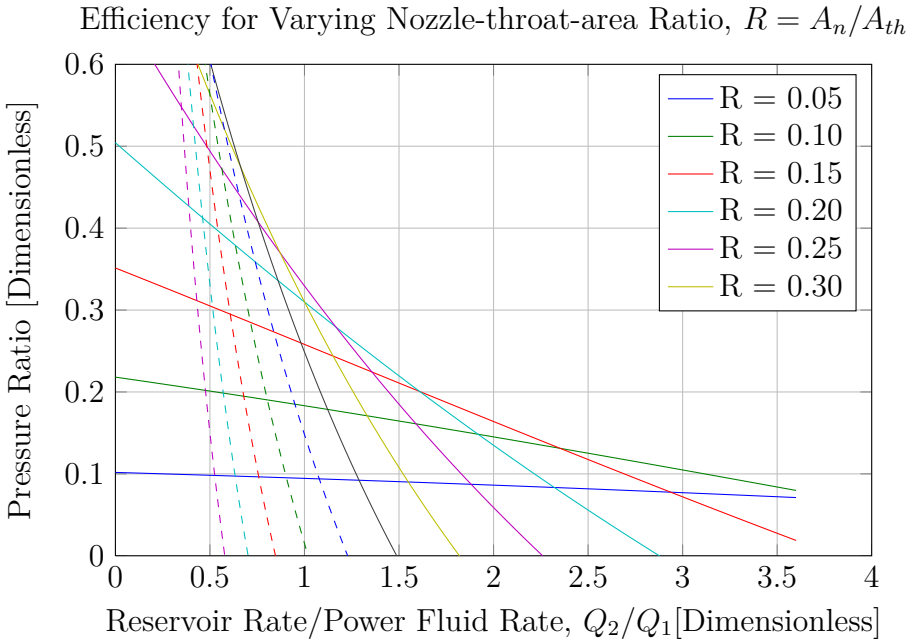

FIGURE B.1: Pressure Ratio for Varying Nozzle-throat-area Ratio

The belonging efficiency plot is shown in Figure B.2. The efficiencies are moving rightwards as the nozzle-throat-area ratio is decreasing.

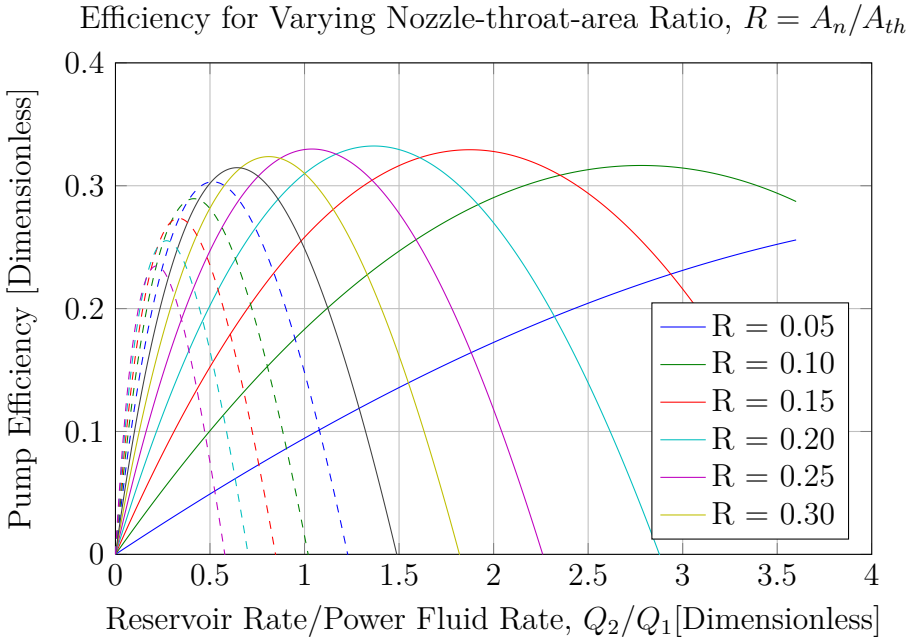

FIGURE B.2: Efficiency for Varying Nozzle-throat-area Ratio

B.2 Incompressible Program Sensitivity

A short program simulating a simple well is attached in Appendix F.1.2. This program assumes no friction losses in the well, which obviously is not realistic. The purpose of this section was to review some effects changing properties related to well and jet pump have on the well pressure.

The mixture density, downstream pump, is calculated in the following manner, recalling that $M = Q_2/Q_1$.

$$\rho_3 = \frac{\rho_1 Q_1 + \rho_2 Q_2}{Q_3} = \frac{1}{1+M}\rho_1 + \frac{M}{1+M}\rho_2 \tag{B.4}$$

As the pump is lowered in the well a small pressure variation is seen at surface (Figure B.3). This difference is due to increased hydrostatic pressure as the depth increases and more power fluid is pumped. In addition, there is reduced lubricity due to increased amount of water, given that water is used as power fluid. This would aggravate the situation, and the plot would be shifted leftwards.

In Figure B.4 the surface pump pressure is changing. The effect is a increased diffuser pressure at the pump depth. This imply that changing power fluid pressure can be used to regulate the wellhead pressure for the same reservoir and power fluid rate.

In Figure B.5, the reservoir pressure is changing. This could be the case as the reservoir is depleted, or injection near the well influence the reservoir pressure experienced by the well. The pressure increase propagates to surface.

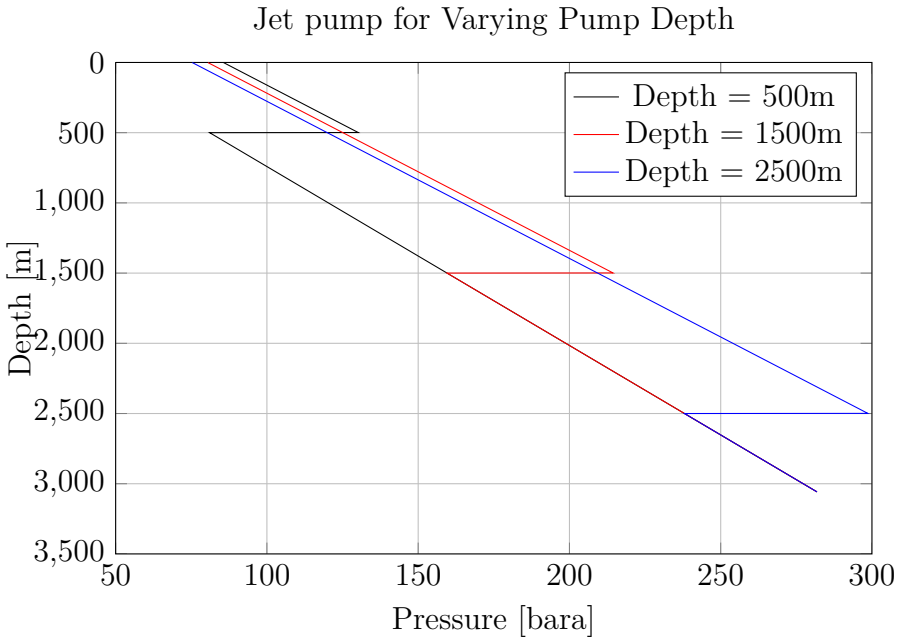

FIGURE B.3: Well Pressures for Varying Depths

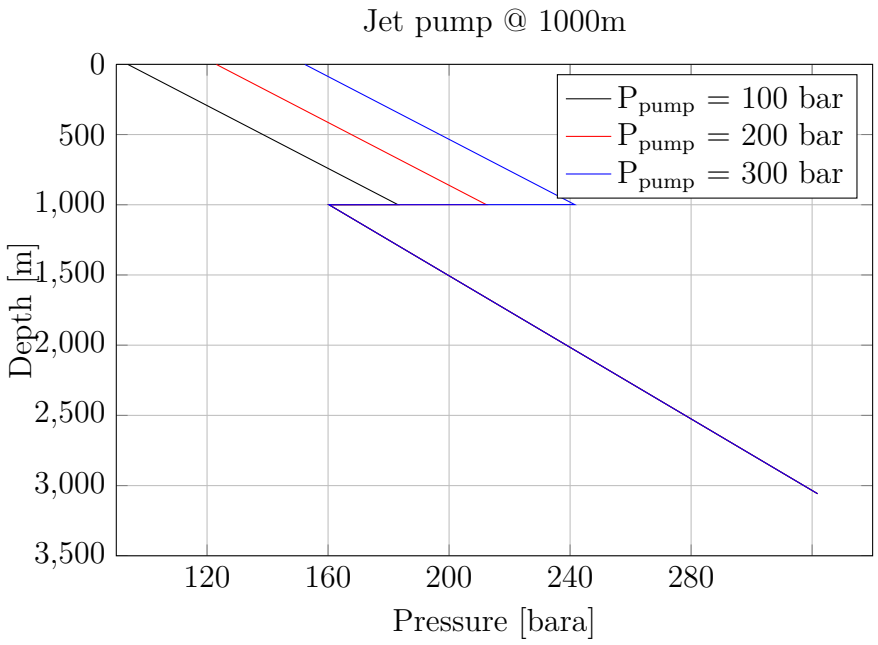

FIGURE B.4: Well Pressures for Varying Power Fluid Pressures

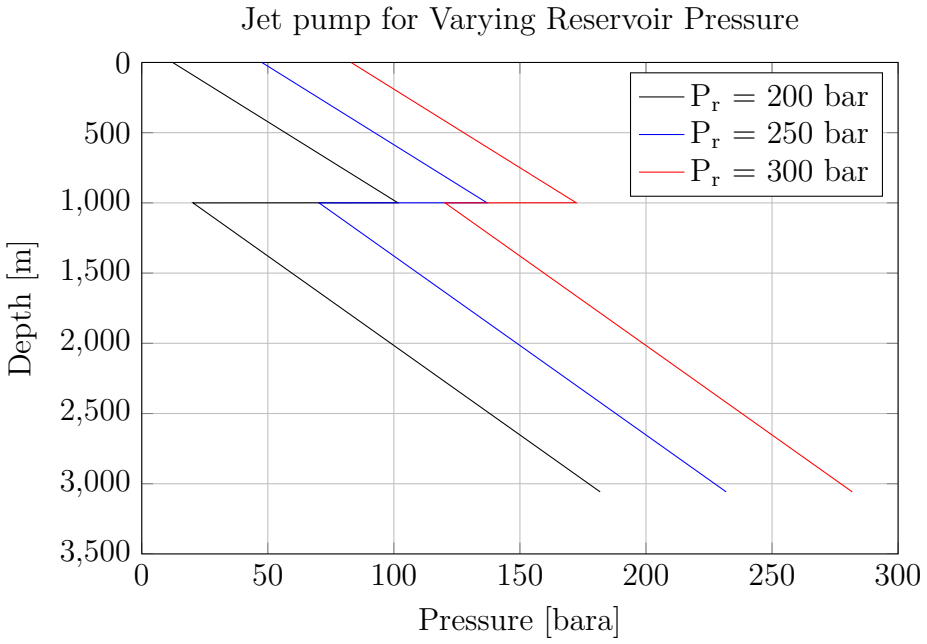

FIGURE B.5: Well Pressures for Varying Reservoir Pressure

Appendix C

Field Applications

C.1 Vega field, Sicily

The Vega field, offshore Sicily, is a 15 °API oil. The field is one of the biggest heavy oil fields in Italy. Figure C.1 show the completions used at Vega and Gela.

The partners recognized jet pumps as a cheaper artificial lift method and tested various jet pump sizes, types and rates of power-fluid. They concluded that jet pumps can be set in the production string by wireline or coiled tubing. Run-in-hole (RIH) and Pull-out-of-hole (POOH) can also be performed by direct or reversed fluid circulation through the slide door valve.

Riva et al.[17] found that system tests confirmed a very low system flexibility, verifying that being reported in the literature. By low flexibility one meant that the jet pump was fit for certain specifications when it came to power-fluid and reservoir rate, reservoir pressure, amount of gas etc. Jet pump sizing were mainly done at surface, which meant that continuous changes in downhole conditions were challenging to address. To minimize the operational difficulties, such as scaling, plugging and paraffin creation, it was important to select the biggest nozzle-throat-area combinations from those available.

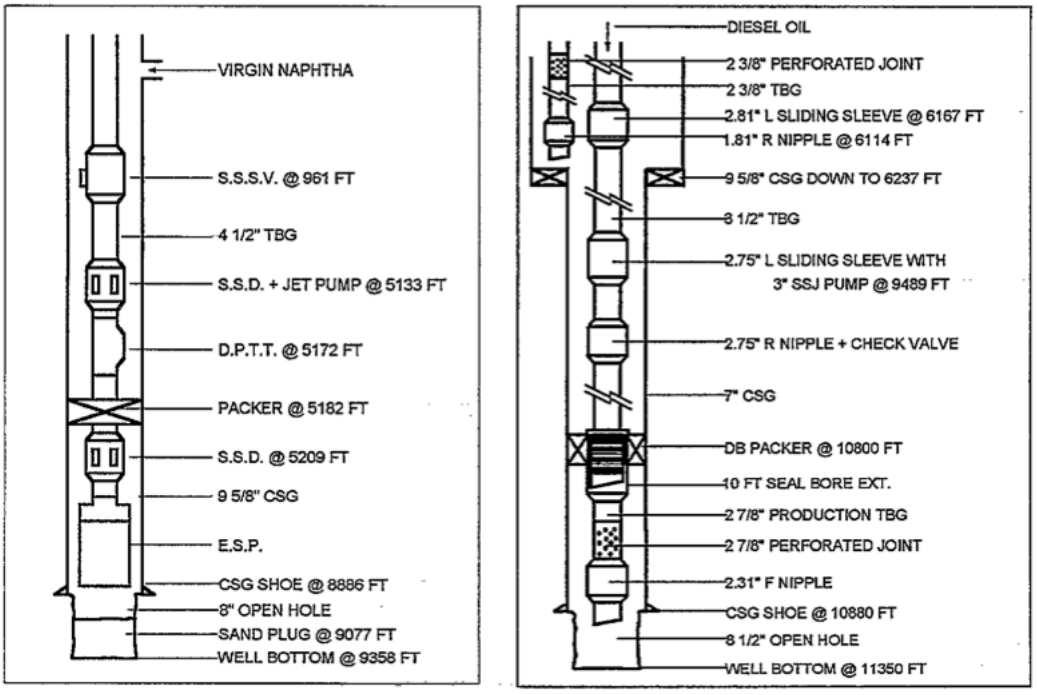

FIGURE C.1: Vega and Gela Completions

Vega field is a fractured carbonate reservoir, exploited by means of a fixed platform. Although some of the wells were initially flowing with a high Productivity Index (PI), the expected Water-Cut (WC), along with the demand of increased flow rates, favored using Electrical Submersible Pump (ESP) when the wells were completed.

As the ESP-systems started to fail it became necessary to retrieve and replace these. Due to decreasing field production a study was carried out to find suitable replacements. Jet pumps were selected because they were possible to place with wireline inside the landing nipple profile of the sliding-side-door (SSD). This meant that the jet pump could be retrofitted and landed where the ESPs previously were located. The operator chose Naphta as power fluid and list the following arguments for their selection.

- Liquid density reduction in production string.
- Less frictional losses due to reduced viscosity of produced fluids.
- Less frictional losses due to instantaneous and better mixing of power and well fluid in jet pump throat.

- Increased head delivery by pump

C.2 Kuparuk Field, Alaska

The Kuparuk field is located at the Northern slope of Alaska, and is the second largest oil field in the area. The jet pumps installed apply formation fluid as power source. By this, the jet pumps exploit the natural energy of a highly productive zone to boost production from a less productive zone. In addition, gas injection is possible in these wells because annulus above the upper production packer is not in use. Simultaneous gas injection, along with jet pumping, further boost the production. Peirce et al.[40] reports that Formation Powered Jet Pumps (FPJP) are easy to install with rapid payout periods, often measured in days. Wells are normally completed with straddle completions to provide isolation between the two layers (Figure C.2). The sliding sleeve completion is also recognized as a possible way of completing the well (Figure C.3).

To get the appropriate jet pump sizing, static bottom hole pressure of each sand layer was measured. Pressure data and production logging data from each zone were input to the FPJP design algorithm. Since the jet pumps are formation powered, awareness of changing reservoir fluid properties in both zones is crucial. It has been reported that it is necessary to provide a stable pressure support to the FPJP wells. If the pressure is not maintained it is difficult to keep the performance within the envelope the jet pump was designed for.

C.3 Hay Project, Western Canada

The Nexen Hay River Bluesky oil pool is one of the biggest discoveries in Western Canada in the past few decades. The oil exploited is a medium to heavy oil (15 °API). Because of the remote location, beneath a very flat muskeg area, the artificial lift method chosen had to be extremely reliable. In addition, the method

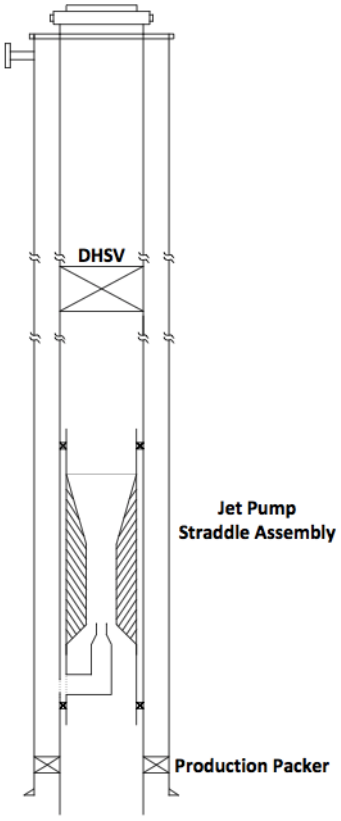

FIGURE C.2: Straddle Assembly (Courtesy: PTC)

had to be safe and capable of lifting large volumes of fluid with a significant drawdown. It was also a criteria that the method was able to operate successfully in extreme deviations in "build" sections of the development wells.

As power fluid they used both produced fluids and water. Problems with cavitation were reported while using produced fluids. With this scheme the only additional cost of running the jet pump was to ensure sufficient pipelines and horsepower to boost the stream. Anderson et al.[33] reported that even though the jet pump had considerably higher horsepower requirements, the jet pump was still the preferred artificial lift option. The jet pump was landed 10-20 meters above the formation, at 323 meter true vertical depth, in the 70 ° build section. The capability of placing the jet pump at high angle is attractive because the pump may be placed close to the formation. This allows maximum drawdown of each well.

The jet pump in Figure C.4 is a typical jet pump used at Hayriver. It is landed in a pump seat, located in the tubing string close to the casing shoe. Jet pump

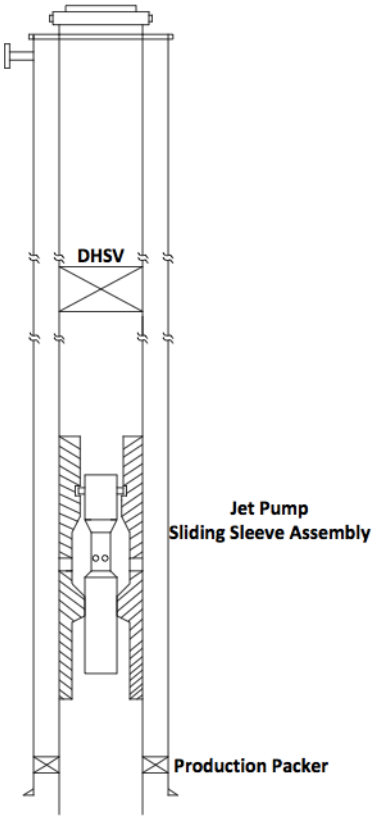

FIGURE C.3: Sliding Sleeve Assembly (Courtesy: PTC)

activation happen by pumping high-pressure power fluid down the tubing.

The benefits have been reported as being quite similar to the other cases. The disadvantages have been specifically mentioned to be

- Lower efficiency compared to other pump systems, requiring considerably more horsepower
- High volume of fluids require large surface facilities
- High dependency upon backpressure

Anderson et al.[33] recommends that this artificial lift option should be considered in cases where high volume lift is an absolute necessity. Detailed pre-project planning is extremely important to ensure that facilities can accommodate the expected volumes.

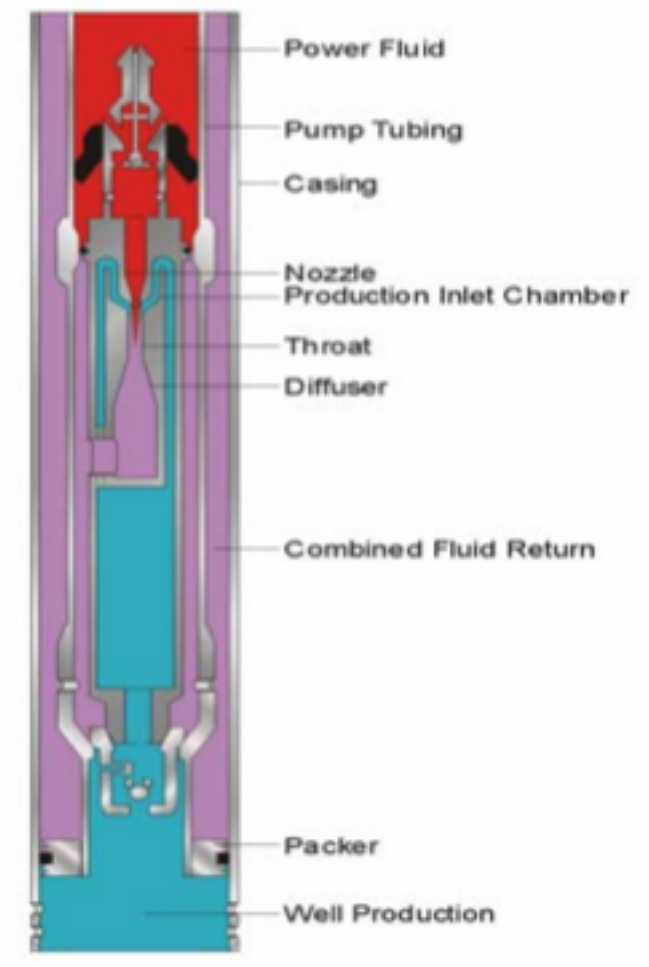

FIGURE C.4: Hay Project Jet Pump

Appendix D

System Description

D.1 Jet Pump

Jet pumping is a type of artificial lift, with no moving parts. For this reason it is recognized to be more durable than e.g. Electrical Submersible Pumps (ESPs). ESPs are high efficiency pumps, but vibration and fluid schemes may reduce their lifetime. However, in some cases they have operated over longer time. In general the lifetime of rotational equipment is limited. Jet pumps, due to robust design, have a considerably longer lifespan than ESPs.

When it come to design it is particularly important to make the exposed parts out of durable materials, such as Tungsten Carbide. Exposed parts are the parts where high velocity flow occur, mainly in nozzle, throat suction and throat. The power fluid is most likely quite clean, but can still contain particles. By using robust materials there is reduced demand for retrieving the pump for maintenance. Erosion and corrosion could possibly be a considerable problem in wells with H_2S-rich formation-water and sand producing wells[35].

D.2 Well Barriers

In NORSOK (Norwegian Continental Shelf safety regulations) D-010[41] a well barrier is generally defined as:

> *Envelopes of one or several dependent well barrier elements (WBEs) preventing fluids or gases flowing unintentionally from the formation, into another formation or to surface.*

Further it is stated that well barriers shall be defined prior to commencement of an activity or operation by description of the required WBEs to be in place is a specific acceptance criteria.

This mean that the barriers necessary when installing a jet pump must be described. Since we are in production mode, the chapter on production barriers is necessary to investigate further. We have a well circulating fluid through annulus which make the most similar case described in NORSOK a "Typical gaslift platform production well".

From Figure D.1 we see that the primary well barriers are:

- Production packer
- Annulus surface controlled sub-surface valve (ASCSSV)
- Surface controlled sub-surface safety valve (SCSSV)
- Casing (Between ASCSSV packer and production packer)
- Completion string (between ASCSSV and SCSSV)

All these barriers have to be present in order to safely operate a system with a jet pump. Further NORSOK states, about multipurpose wells, that transport medias, in both tubing an annulus, will be subject to monitoring of the B-annulus. This means that annulus must be monitored at all times to detect leakage. C-annulus is then subject to periodical surveillance. Also, if the production casing

8.8.2 Typical gaslift platform production well

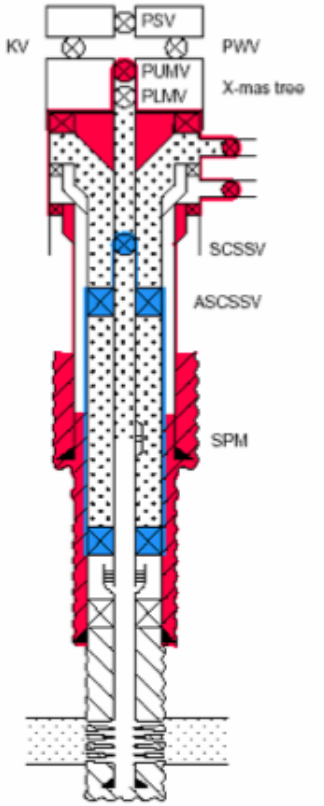

Well barrier elements	See Table	Comments
Primary well barrier		
1. Production packer	7	
2. Casing	2	Between ASCSSV packer and production packer.
3. ASCSSV	9	
4. Completion string	25	Between ASCSSV and SCSSV.
5. SCSSV	8	
Secondary well barrier		
1. Casing cement	22	Production casing cement.
2. Casing	2	Production casing and casing into intermediate casing.
3. Casing cement	22	Intermediate casing cement.
4. Casing	2	Intermediate casing.
5. Wellhead	5	Intermediate casing hanger w/seals.
6. Tubing hanger	10	
7. Annulus access line and valve	12	Tubing head w/annulus gas injection line w/valve.
8. Surface production tree	33	W/master valve.
9. Annulus access line and valve	12	B-annulus access line w/valve.

Note
None

FIGURE D.1: Gas Lift Production Well

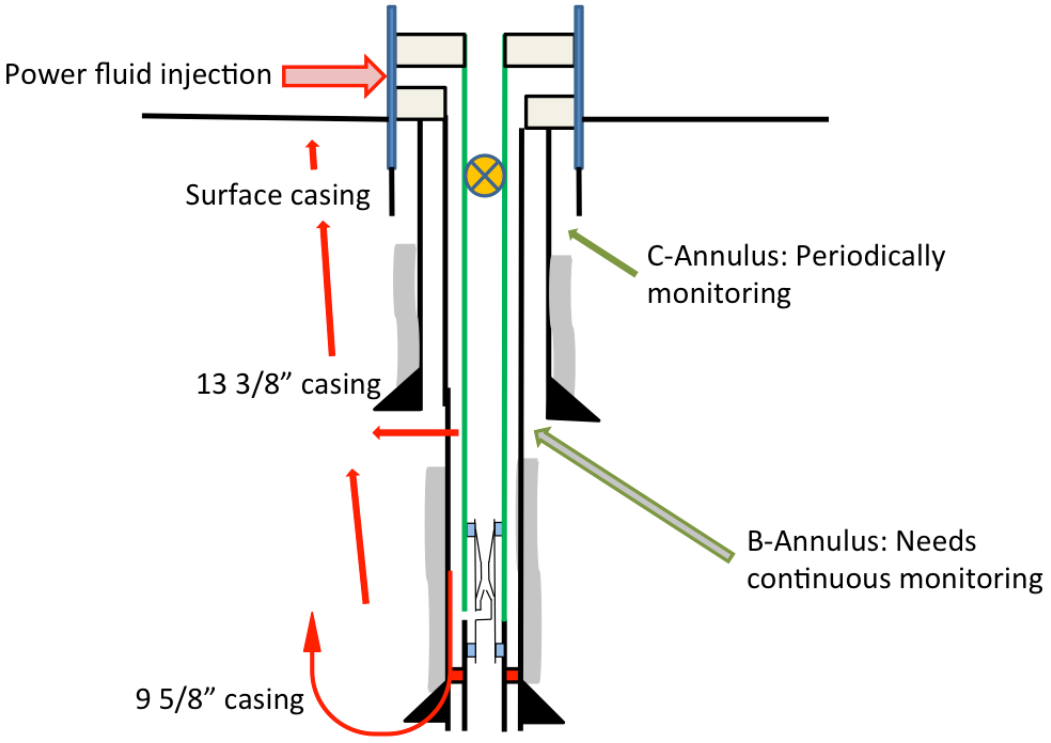

FIGURE D.2: Possible Leak Paths

is not cemented into the intermediate casing, the exposed formation shall have a documented ability to withstand a leaking production casing scenario. Figure D.2 show a typical well with possible leak paths included.

Here are some possible ways to reinstate the barriers necessary to produce.

1. *Jet Pump over Downhole Safety Valve (DSV)*: Downhole safety valve is approved as a barrier. Considering a case where we want to lower the pressure somewhat, a jet pump installed above DSV could solve barrier issues. The DSV could be closed during maintenance, preventing reservoir fluid flowing into annulus

2. *"Safety valve" in Jet Pump Assembly*: A valve operating in the same manner as a DSV in the jet pump assembly could provide the necessary barrier. There are hydraulic issues as the jet pump position is lowered in the well.

3. ÂăDual string: A dual string with a valve at the bottom could provide the barrier. Annular packers prevent flow up annulus above the valve.

4. *Annular Safety Valve*: In a recompletion, or a well with annular safety valve (ASV), the barrier necessary is in place. Lost pressure from surface would safely seal off annulus, and prevent reservoir fluids from migrating upwards.

The jet pump can be installed in the well by two methods. The first method is to run the jet pump with wireline and install it by plunging a hole in tubing. Alternatively, the jet pump may be installed by pulling the completion, and re-complete the well with a sliding sleeve with landing nipples to accommodate the jet pump. The jet pump may then be installed by wireline. If the well is completed with a side pocket mandrel, e.g. if the well has been used for gas lift, a jet pump may be fitted to land there.

D.3 Straddle Assembly

If the completion is not to be retrieved, a through tubing installation of the jet pump is possible. This may be done either by setting the assembly across a side pocket mandrel (Figure D.3), if present, or across open hole punched in tubing (Figure D.4). The intervention is categorized as light intervention, and can be performed by wireline or coiled tubing. This demands less equipment at surface during installation than a heavy intervention. The cost is also considerably less for a wireline operation. This assembly type is a bore, containing the jet pump, set inside the tubing. The assembly seals off the open annulus by packers above and below the jet pump. Hence, the well fluids are forced into the throat.

The annulus is filled with power fluid, and flows into the nozzle through the sliding sleeve or the plunged hole. As long as annular pressure exceeds tubing pressure there is no danger of reservoir fluids entering the annulus. A problem arise when the power-fluid pump is down for some reason, then the possibility of formation fluid entering annulus is present. The critical factors are then:

- Burst criteria of casing

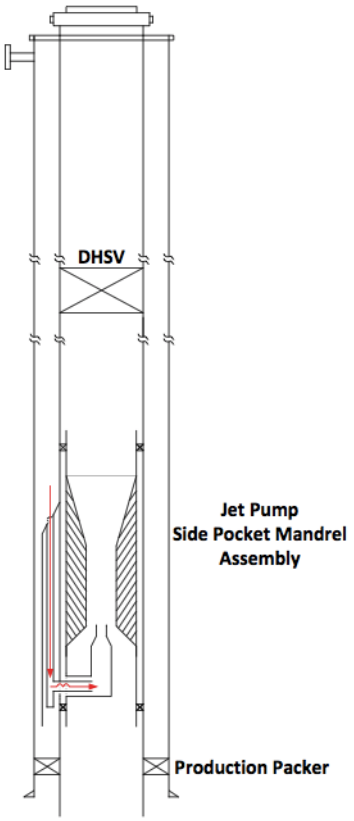

FIGURE D.3: Straddle Assembly, Mandrel Type

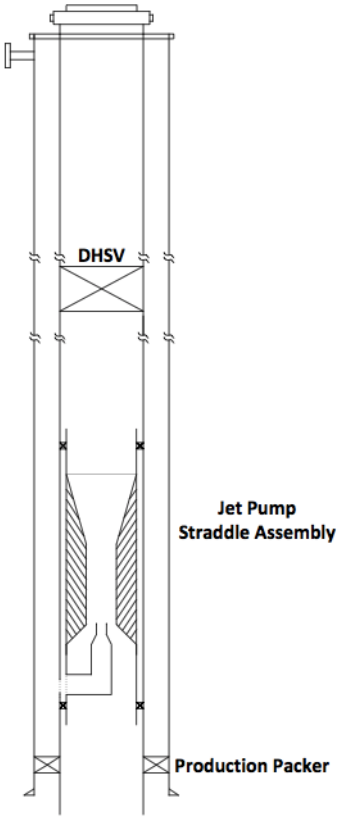

FIGURE D.4: Straddle Assembly, Open Hole Type

- Formation strength

The casing burst criteria is normally 40% gas-filled hole. If the amount of gas entering the annulus exceeds this limitation, there is a risk of casing burst.

Another factor is the formation strength. The pressure in annulus may increase by such an amount that the fluid gradient exceeds the fracture gradient. An underground blow-out is difficult, if not impossible, to control. The cement strength, or a poorly performed cement job, may also be a path for the gas to seep towards the surface. If this happens, it is almost impossible to regain control and stop the influx of gas. Figure D.2 show possible leak paths for gas.

It is crucial to control fluid flow from reservoir during revision stops or other unplanned downtimes. The challenge to safely seal off the annulus during downtime have to be assessed before a jet pump-assembly is installed in a platform well.

D.4 Sliding Sleeve Assembly

The other alternative is to use a sliding sleeve completion (Figure D.5). This mean that the flow path to annulus is provided by the opening and closing of the sleeves. Slickline tool may be used to close the sleeve[42].

To install this, if a sliding sleeve assembly is not already present, demands a heavy intervention. The completion has to be pulled in order to set the sliding sleeve as part of the completion, which is expensive and time consuming. It has been recognized by platform operators [43] that if the well is first completed with ESP, a sliding sleeve jet pump is favorable to install in order to continue production when the ESP has shut down.

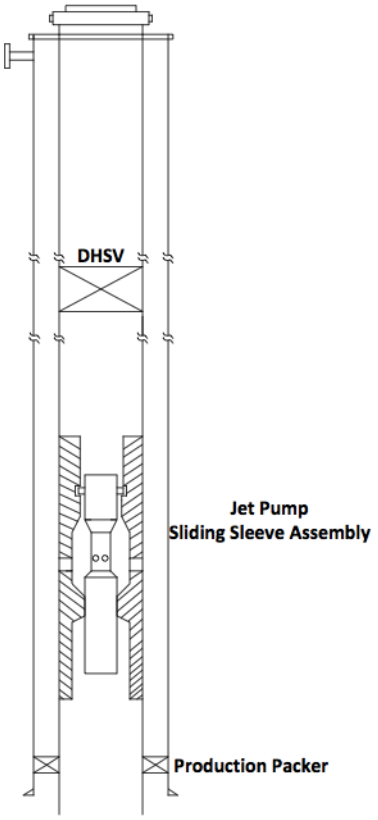

FIGURE D.5: Sliding Sleeve Assembly

D.5 Operational Restrictions

The depth which the jet pump can be installed, and factors that restrict this is mainly dependent on:

- Tubing restrictions
- Suction pressure available

Placement in Well

Figure D.6 show the hydrostatic pressure of the reservoir fluid column. Initially the well is produced by choking back reservoir flow. As the reservoir pressure is depleted, the driving pressure available to lift reservoir fluids to surface is decreasing. The figure show two cases; the right one when the reservoir pressure is just sufficient to lift the fluids to wellhead. The left show a hypothetical case when the

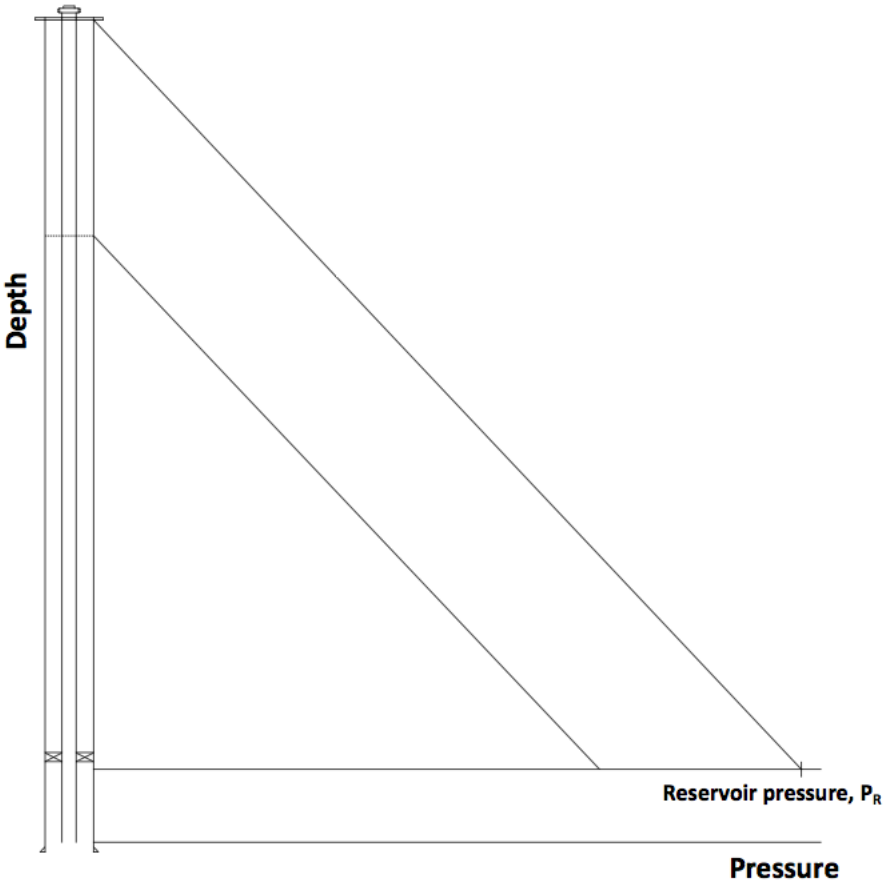

FIGURE D.6: Well Without Jet Pump

reservoir pressure has been depleted to an extent that the natural reservoir energy is not sufficient to lift the reservoir fluids to surface any longer. The practical implication of this figure is that if there is no pressure support from reservoir, the depth the jet pump is set, is critical for the production. The power-fluid only contributes to add energy above the jet pump. It is reservoir driving pressure that lift reservoir fluid to the jet pump. If the jet pump is set high, the reservoir pressure has to be maintained in order to keep the well hydraulically alive. Consequently, the maximum depletion possible from a reservoir is increasing with installation depth.

The fraction of gas is dependent on the oil bubble point. If the pressure drop beneath the bubble point, gas is liberated. The efficiency is decreasing as free gas is introduced to the jet pump[34]. However, free gas reduces hydrostatic pressure in the well. It is beneficial to place the jet pump sufficiently deep to avoid free gas in the jet pump.

Clegg et al.[44] state that other limiting factors for setting depth is power-fluid pressure or horsepower. Because of the relatively short assembly length, and no parts that are exposed to vibrations, as for an ESP, there are no constraints regarding dog-leg angle.

There is a constraint when it comes to annular packers. Normally, above every reservoir zone there is a production packer that prevents reservoir flow in annulus. The jet pump has naturally to be set above these.

Annular limitations

The power-fluid is circulated through annulus, and it is important that limitations on casing, tubing and annulus are not exceeded.

The first limitation is the casing burst pressure. If this pressure is exceeded the casing can burst and the well integrity is compromised.

Differential pressure between power fluid in annulus and reservoir fluid in tubing might get to high. This differential pressure may cause tubing collapse.

Another constraint is the formation strength. If the annular pressure exceeds the formation strength, the formation could fracture and an undesirable leak-path is possibly established.

There is also a possibility of leakage of reservoir fluids between casing and cement. This might be due to a poor cement job or movements of formation relative to casing.

Appendix E

Program Modeling Procedures

This chapter is given for several reasons. The chapter offers a detailed description of the modelling procedure. This will be beneficial if the work will be used in the future. The chapter also offer additional information for readers interested in the developing procedure. The chapter also make the program transparent and easier to understand.

E.1 Matlab-program

Matlab was chosen to build the equations presented in Chapter A.1. The code is attached in Appendix F.2.1. There are four equations (equation A.2, A.7, A.9 and A.11) defining the jet pump performance. The first equation is solved independently of the others, and calculates the jet dynamic pressure, Z. With the jet dynamic pressure the other equations can be solved simultaneously, using the Matlab function called Fsolve. Fsolve is a MathWorks tool[45] that find roots (zeroes) to a system of nonlinear equations. The problem is formulated as.

$$F(X) = 0 \tag{E.1}$$

Where $F(X)$ is a function that returns a vector with the solution values. The equations have to be written on the form

$$f(x) = 0 \tag{E.2}$$

The problem is solved when the equality, or approximation, in equation E.1 is solved. The three equations was thus formulated in the following manner.

$$f(1) = (\tfrac{Q_2}{Q_1})(p_s - p_o) + p_s\phi_s ln(\tfrac{p_s}{p_o}) - Z\frac{S(\frac{Q_2}{Q_1}) + \gamma\phi_s}{c^2}(1 + K_{en})((\tfrac{Q_2}{Q_1}) + \phi_s\frac{p_s}{p_o})^2 \tag{E.3}$$

$$\begin{aligned} f(2) = (p_o - p_t) - ZR^2(2 + K_{th})(1 + S(\tfrac{Q_2}{Q_1}) + \gamma\phi_s)(1 + (\tfrac{Q_2}{Q_1}) + \phi_s\frac{p_s}{p_t}) \\ + 2ZR + 2Z\frac{R^2}{1 - R}(S(\tfrac{Q_2}{Q_1}) + \gamma\phi_s)((\tfrac{Q_2}{Q_1}) + \phi_s\frac{p_s}{p_o}) \end{aligned} \tag{E.4}$$

$$\begin{aligned} f(3) = (p_d - p_t) + \frac{p_s\phi_s}{(1 + (\frac{Q_2}{Q_1}))}ln(\frac{p_d}{p_t}) - ZR^2\Big\{\frac{1 + S(\frac{Q_2}{Q_1}) + \gamma\phi_s}{(1 + (\frac{Q_2}{Q_1}))}\Big\}\times \\ \Big((1 + (\tfrac{Q_2}{Q_1}) + \phi_s\frac{p_s}{p_t})^2 - a^2(1 + (\tfrac{Q_2}{Q_1}) + \phi_s\frac{p_s}{p_d})^2 - K_{di}(1 + (\tfrac{Q_2}{Q_1}) + \phi_s\frac{p_s}{p_t})(1 + (\tfrac{Q_2}{Q_1}))\Big) \end{aligned} \tag{E.5}$$

The problem is solved by calling the solver starting at some initial vector X_0. Fsolve use the functions tangent and seeks a solution to the problem. The solution vector, X, returns the set of variables that solves the problem. The variables are defined as.

$$X = \Big[Q_2, p_o, p_t\Big] \tag{E.6}$$

For convenience the start vector take the following input as a first guess for the solution algorithm.

$$X_0 = \left[Q_1, p_s, p_d\right] \tag{E.7}$$

The reason for choosing these start values is that the solution, by theory, must be located close to the starting values. It is known that the throat-inlet pressure is somewhat lower than the suction pressure, p_s. Similarly, the throat-outlet pressure and reservoir rate are normally close to diffuser pressure, p_d, and power fluid rate, Q_1, respectively.

The rest of the necessary parameters are defined inside the function named 'nleq'. The only parameters that are fed to solvers are the function name and the initial vector, X_0. Passing all parameters to the solution algorithm would be the most advantageous, but this is somehow complicated and the implementation was not pursued. Figure E.1 show a flow chart on how the Matlab program work. Every parameter necessary to be defined inside 'nleq' is shown. The Mathworks solver Fsolve[45] is called by

$$X = fsolve('nleq', X_0) \tag{E.8}$$

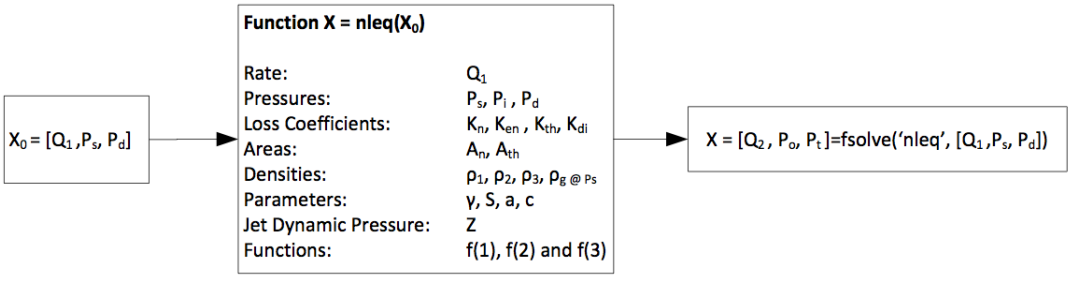

FIGURE E.1: Matlab Program Flowchart

The returning vector contains the solution of the problem for the initial conditions along with a report summarizing possible notifications of errors. The drawback of this program is that it lacks the capability of communicating with Prosper.

Running multiple wells would be tedious as every parameter would have to be redefined for each well. The Matlab code is therefore suitable for isolated jet pump calculations, which is practical if the goal is to study jet pump performance.

E.2 C#-Program

When a working Matlab-program had been developed, a change in programming language was necessary to ease the further work. The code built in Matlab was transformed to suit the C#-language and necessary solution algorithms were introduced to get the same behavior as the Matlab-program. The program was first run isolated in a test section to verify that the performance was comparable with the Matlab results. Afterwards, the model was connected to Prosper in a way that the program communicated variables back and forth necessary to perform desired calculations.

Isolated Program

Building the program in C# was challenging, and extensive knowledge about programming was necessary. Gisle Otto Eikrem helped building the model. Model performance was in cooperation verified assuring that errors and mistypings had been avoided. A brief calculation procedure explanation is given in the following paragraph.

Each variable was defined in a Parameter Dictionary, which was necessary because the algorithm solve the system of equations by algebra. When calculations are required the program acquire the belonging values from the dictionary. The three equations, Equation A.7, A.9 and A.11, were formulated the same way as the Matlab problem, such that $f(x) = 0$. Every parameter was referred to through the Parameter Dictionary except the variables, Q_2, p_o and p_t which were denoted by X, Y, and Z. Since the equations were to be used several times, as is the nature of iterative routines, the functions were compiled. A first guess, X_0, was defined

as the Alglib[46] package âĂŸNLEQâĂŹ was entered. In this package the solver took several necessary parameters as input to solve the problem. These parameters were the variables, convergence criteria, maximum number of iterations, maximum step length etc.. The calculated solution and a report, summarizing number of iterations and termination type, was output.

A technical description is given in Table E.1. The stepwise procedure summarize, and briefly explains, each necessary step to make the program runnable.

Table E.1: Isolated Program Procedure

Step	**Description**	
1	Parameter Dictionary	Define parameters. This includes all parameters except the variables
2	Define Variables	$X = Q_2$, $Y = p_o$ and $Z = p_t$
3	Define Functions and Compile	Defining functions based on equation exchanging the three variables with X, Y and Z. Thereafter compiling the equations
4	Initialize X_0	âĂIJFirst guessâĂİ, as specified for the Matlab code
5	NLEQcreatelm()	Initialize algorithm state defining dimensions, starting point and a reference to the structure that stores the equations
6	NLEQsetcond()	Define the convergence criteria and the maximum number of iterations allowed
7	NLEQsetstpmax()	Define maximum step length allowed for the routine
8	NLEQsetxrep()	This command turns on/off reporting. Beneficial to verify termination type and number of iterations
9	NLEQsolve()	Solver for the NLEQ. This function has the structure reference, the function and the Jacobian as input
10	NLEQreport()	Calls the report from run performed
11	NLEQresults()	Report results from the numerical solver

The function and the Jacobian matrix had to be defined seperately outside the program, and were subsequently called when needed. The function defines the variables, and thereafter evaluates each function defined in Step 3. The convergence criteria is defined as a squared-function. This way, convergence is obtained when the following criteria is satisfied

$$F = f_1^2 + f_2^2 + f_3^2 < \epsilon \tag{E.9}$$

ϵ is set to some small value in the order of 10^{-6}. The Jacobian matrix is on the following form

$$J(Q_2, P_o, P_t) = \begin{pmatrix} \frac{\delta f(1)}{\delta Q_2} & \frac{\delta f(1)}{\delta p_o} & \frac{\delta f(1)}{\delta p_t} \\ \frac{\delta f(2)}{\delta Q_2} & \frac{\delta f(2)}{\delta p_o} & \frac{\delta f(2)}{\delta p_t} \\ \frac{\delta f(3)}{\delta Q_2} & \frac{\delta f(3)}{\delta p_o} & \frac{\delta f(3)}{\delta p_t} \end{pmatrix} \tag{E.10}$$

The Jacobian Matrix calculates the gradient of a function at a given location. Each function is partially derived with respect to the variable set (Q_2, p_o and p_t) by the Autodiff package. Autodiff[31] utilize automatic differentiation, which exploits the fact that all computer programs calculate a sequence of elementary functions and arithmetic expressions. The automatic differentiation apply the chain rule multiple times to calculate the function derivative. The reason for chosing automatic differentiation is that changes in the function expression automatically change the derivative. By doing this the chance of misprinting is reduced, which is beneficial compared to a symbolical differentiation were it is necessary to compute a new derivative by hand. Automatic differentiation is also believed to be very accurate. The idea is shown in Figure E.2

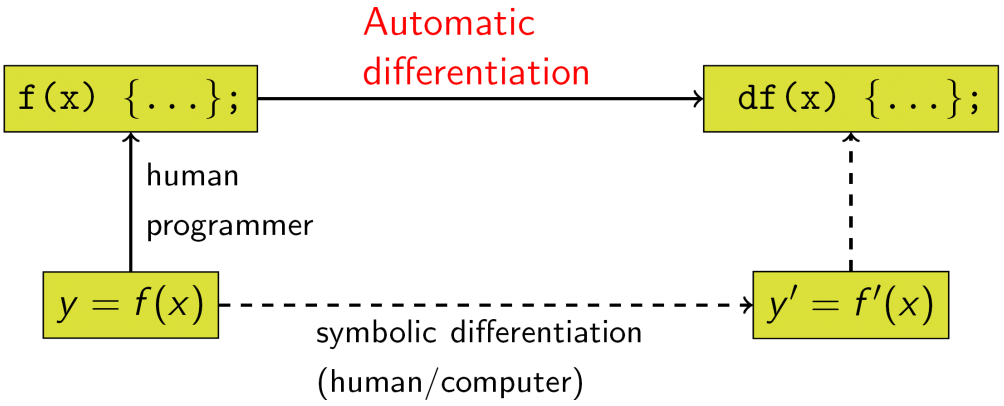

FIGURE E.2: Automatic Differentiation

The alternative could be to implement a numerical solver such as the Newton-Raphson. Newton-Raphson has the same functionality except that it approximates

the derivative in a given point rather then calculating it explicitly. Gradient calculations, explicitly or numerically, are normal in solvers such as the one being used in this case. Alglib utilize a numerical solver called the Levenberg-Marquardt-like nonlinear solver[47]. The solver is a popular choice in least squares curve fitting and for nonlinear programming. The user provide a minimization problem and guess a reasonable starting point. The method dampen the contributing factors to minimize the problem.

E.3 Implementation of Cunningham's Jet Pump

Prosper solve the jet pump system in the following manner[20]:

1. With specified surface injection pressure and rate a calculation is performed to find delivery rate and pressure at nozzle.
2. From inflow performance (IPR) the bottomhole pressure is found, and a co-current calculation to jet pump suction is performed.
3. Counter-current calculation from wellhead pressure downhole with the combined rates.

This way of solving the problem was pursuit. Prosper has a gradient package that solely calculate the well with specified inlet conditions. This could be used to calculate the two pipe segments. The idea was implemented with the self-built routine, as shown in Figure E.3.

Reservoir rate is the iteration parameter and it is varied until the system converge for desired wellhead pressure and power fluid rate and pressure. The idea is presented in Figure E.4. A simultaneous solution is necessary to find the criteria such that the

$$p_{d,Jet\ Pump\ Calculated} \approx p_{d,Counter-Current} \tag{E.11}$$

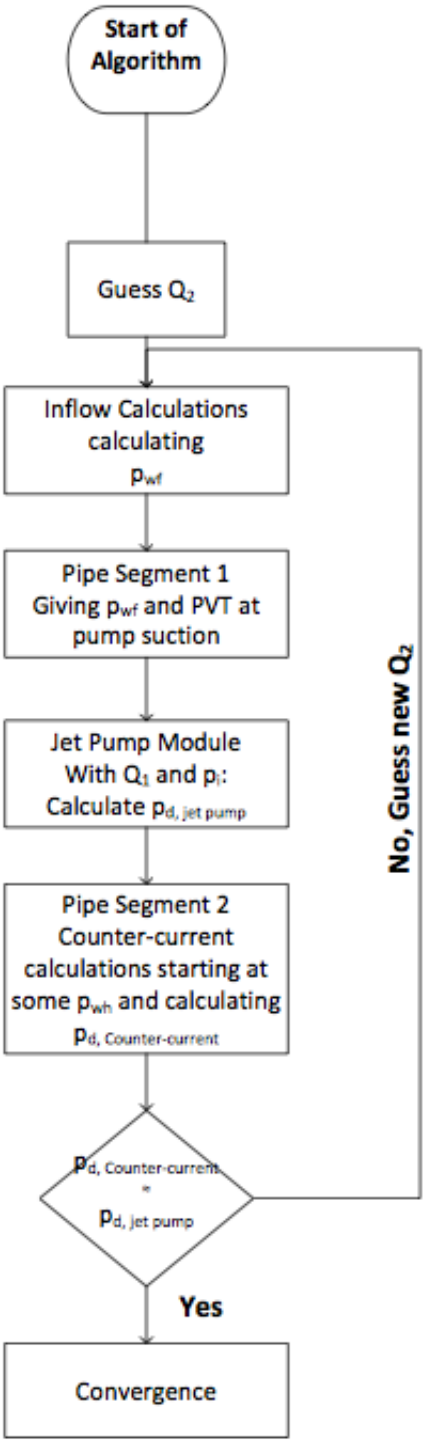

FIGURE E.3: Flow Chart of Well with Three Modules

Pipe Segment 1

The first pipe segment is from reservoir to jet pump suction. A reservoir rate is chosen and the bottomhole flowing pressure, p_{wf}, is calculated.

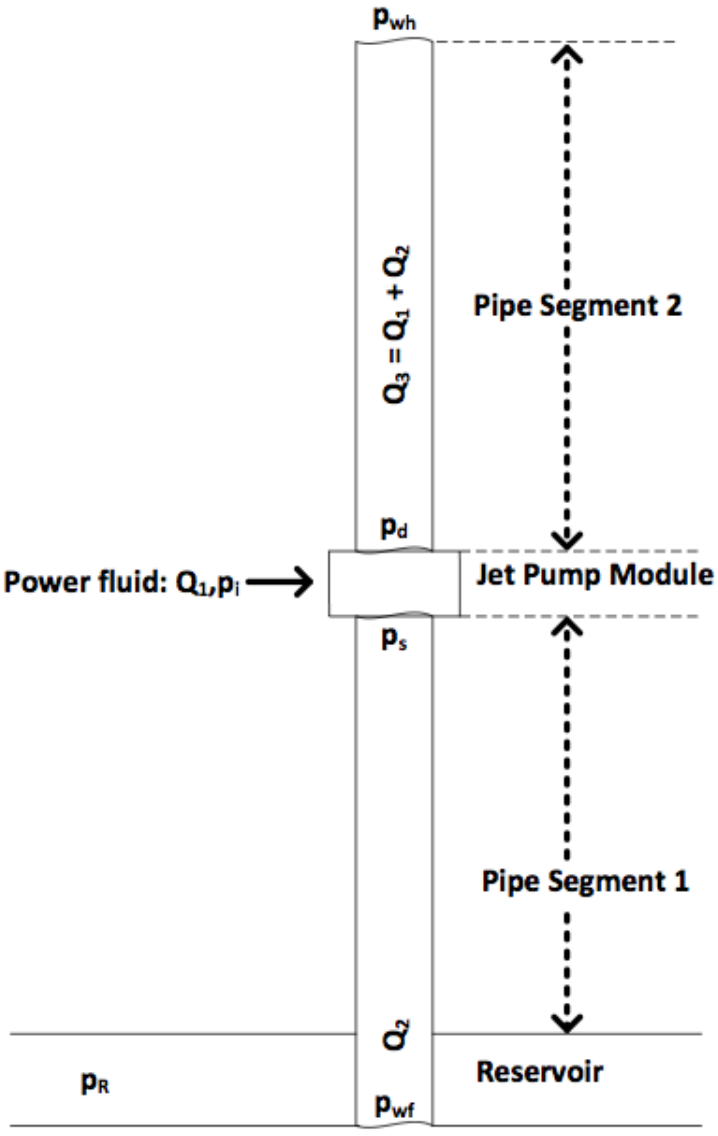

FIGURE E.4: Sketch of Well with Three Modules

$$p_{wf} = p_r - \frac{1}{PI} Q_2 \tag{E.12}$$

For the specified pipe inlet pressure and rate, calculations can be performed towards surface. This is done in the "Gradient Analysis" package in Prosper. The calculations terminate when the calculations have reached the outlet of Pipe Segment 1. The conditions at jet pump suction have now been established.

Power Fluid Calculations

The power fluid is pumped through annulus and enter the jet pump through the nozzle. The nozzle delivery pressure can be formulated as

$$p_i = \Delta p_{pump} + \Delta p_{gravity} + \Delta p_{friction} + \Delta p_{acceleration} \tag{E.13}$$

In this project a few simplifications are done and the nozzle delivery pressure is assumed to be defined by

$$p_i = \Delta p_{pump} + \Delta p_{gravity} \tag{E.14}$$

The weakness of neglecting annular frictional losses could be considerable. This is specially true in cases where the rate is high due to the frictional losses proportionality with velocity squared.

$$\Delta p_f = \frac{1}{2} f \rho \frac{L}{d} v^2 \tag{E.15}$$

To calculate frictional losses in annulus it is necessary with knowledge about the outer tubing diameter and the casing inner diameter. This information may have been omitted in regular Prosper models as A-annulus (Figure D.2) seldom is used for fluid transportation. Obtaining information about these diameters or assuming appropriate values may become necessary if one were to include annular frictional losses.

In Prospers jet pump module, and in this implementation, pump pressure and rate from the surface injection pump is utilized as independent properties. This assumption is not realistic as rate and pressure are interconnected through the pump performance curve, and the equation:

$$P_{pump} = \Delta p_{pump} Q_{pump} \tag{E.16}$$

Kinetic and potential energy of power fluid has now been established and all necessary information is defined to calculate the jet pump performance.

Jet Pump Module

In the first jet pump model implementation the goal was to calculate a rate that satisfied the pressure boundary conditions. At this point, the rate is assumed to be known, so the problem may then be reformulated such that there are three unknown pressures. These are the three pressures at throat inlet (p_o), throat outlet (p_t) and diffuser (p_d). With the inlet parameters defined, both from suction and annulus, the jet pump is calculated culminating in a calculated diffuser pressure, $p_{d,\ Jet\ Pump\ Calculated}$. This pressure increase describe the lift, or head, introduced across the pump.

Pipe Segment 2

The counter-current calculations assume that the rate downstream the jet pump is defined as the sum of the two flows entering the pump:

$$Q_3 = Q_1 + Q_2 \tag{E.17}$$

The mixture properties can be calculated as

$$\lambda_3 = \frac{\lambda_1 Q_1 + \lambda_2 Q_2}{Q_3} = \frac{1}{1+M}\lambda_1 + \frac{M}{1+M}\lambda_2 \tag{E.18}$$

Where λ is a property such as density or gas-oil-ratio (GOR). With a known wellhead pressure, p_{wh}, a countercurrent calculation from surface downhole can be performed ending in a diffuser pressure above the pump, $p_{d,\ Counter-Current}$. This pressure must be equal for the routine to terminate. Physically this point can be

explained as the point at which it is sufficient energy downhole to lift the combined fluids to surface.

The whole well is now described through Prosper and the well hydraulics are thus calculated by a well known software. This is advantageous because the majority of Statoil wells are modelled in Prosper. The necessary input for the jet pump simulator is a Prosper well-file along with power fluid properties (ρ_1, Q_1 and p_{pf}), top side pressure restrictions and other input parameters listed in Table 3.2.

Appendix F

Matlab Code

F.1 Incompressible Equations

F.1.1 Program

```
clearvars
% JP - incompressible reservoir fluid

rho_f = 965; % Reservoir fluid density, kg/m3
rho_pf = 1015; % Power fluid density, kg/m3
B = 0.05:0.05:0.6; % Nozzle/throat area ratio
M = 0:0.01:3.6;
Pi = 450; % Power fluid delivery pressure, bara
Ps = 200; % Reservoir fluid suction pressure, bara
Kn = 0.05; % Nozzle LC
Ken = 0;   % Throat entry LC
Kth = 0.1; % Throat LC
Kdi = 0.1; % Diffuser LC

% Declerations
P_i = Pi.*10^5;
P_s = Ps.*10^5;
P_d = 0;
P_t = 0;
P_o = 0;
N = 0; % Pressure ratio
eff = 0; % Efficiency
Z = 0; % Jet dynamic pressure
S = rho_f/rho_pf; % Density ratio (Reservoir/power fluid)
```

```
% M = Q_2./Q_1; % Liquid/liquid flow ratio Q2/Q1
a = 0; % Ath/Ad (throat/diffuser outlet) 5-8% angle a^2=0 (Cunningham)

Eff = zeros(length(M),length(B));
Presratio=zeros(length(M),length(B));
B = B';
% -- JP Calculations --
for i =1:length(B)
        b = B(i);
        c = (1-b)./b;

Z = (P_i-P_s)./(1+Kn);

P_o = P_s - Z.*S.*M.^2*(1+Ken)./(c.^2);

A1 = 2.*b;
A2 = 2.*S.*M.^(2).*b.^(2)./(1-b);
A3 = b.^2.*(2+Kth).*(1+S.*M).*(1+M);
P_t = P_o + Z.*(A1 + A2 - A3);

P_d = P_t + Z.*(b.^2.*(1+S.*M).*(1+M).*(1-a.^2-Kdi));

N = (P_d - P_s)./(P_i - P_d);
eff = M.*N;
Presratio(:,i) = N;
Eff(:,i) = eff;

end

figure(1)
plot(M,Presratio)
axis([0 4 0 0.6])
title('Pressure Ratio')
legend('b = 0.05','b = 0.10','b = 0.15','b = 0.20','b = 0.25','b = 0.30',1);
xlabel('M')
ylabel('Pressure Ratio')
matlab2tikz('pressureratio.tikz', 'height', '\figureheight', 'width', '\figurewidth');

figure(2)
plot(M,Eff)
axis([0 4 0 0.4])
title('Efficiency')
legend('b = 0.05','b = 0.10','b = 0.15','b = 0.20','b = 0.25','b = 0.30',4);
xlabel('M')
ylabel('Efficiency')
matlab2tikz('effb.tikz', 'height', '\figureheight', 'width', '\figurewidth');
```

F.1.2 Sensitivity

```
Psurf = 200;
% Reservoir Fluid
Q2 = 1000; %Sm3/d
Pr = 300; % bar
PI = 55; % Sm3/d-bar
Rho2 = 800; % kg/m3

% Jet Pump data
Kn = 0.05; % Nozzle LC
Ken = 0;   % Throat entry LC
Kth = 0.1; % Throat LC
Kdi = 0.1; % Diffuser LC
a = 0;
b = 0.25; % Nozzle/throat area ratio
c = (1-b)/b;
M = 0.8;
d = 1000; % Depth of jet pump
Rho1 = 1000; % kg/m3
g = 9.81; %m/s2
S = Rho2/Rho1;
Pwf = Pr - Q2/PI; %bar
Rho3 = (1+M)^(-1)*Rho1+M*(1+M)^(-1)*Rho2;
ReservoirDepth = round(Pr*1e5/(Rho1*g));
Pressure = zeros(ReservoirDepth,2);

% Initializing inflow depth and pressure
Pressure(ReservoirDepth,1) = ReservoirDepth;
Pressure(ReservoirDepth,2) = Pwf;

% --- PIPE SEGMENT 1 ---
for i=(ReservoirDepth-1):-1:d
    Pressure(i,1) = i;
    Pressure(i,2) = Pressure((i+1),2) - Rho2*g*1e-5;
end
% --- JET PUMP ---
Ps = Pressure(d,2)*1e5;
Pi = (Psurf*1e5+Rho1*g*d);
Z = (Pi-Ps)./(1+Kn);
Po = Ps - Z.*S.*M.^2*(1+Ken)./(c.^2);
A1 = 2.*b;
A2 = 2.*S.*M.^(2).*b.^(2)./(1-b);
A3 = b.^2.*(2+Kth).*(1+S.*M).*(1+M);
Pt = Po + Z.*(A1 + A2 - A3);
Pd = Pt + Z.*(b.^2.*(1+S.*M).*(1+M).*(1-a.^2-Kdi));
Pressure((d-1),2) = Pd*10^(-5);
```

```
Pressure((d-1),1) = d-1;
% --- PIPE SEGMENT 2 ---
for i=(d-2):-1:1
    Pressure(i,1) = i;
    Pressure(i,2) = Pressure((i+1),2) - Rho3*g*1e-5;
end
% --- PLOT ---
plot(Pressure(:,2),Pressure(:,1))
axis ij
xlabel('Pressure [bara]')
ylabel('Depth [m]')
title('Jet pump @ num2str(d) m')
title([ 'Jet pump @ ' num2str(d) 'm']);
%text((Pd*10^(-5)-20),d+100,'Jet Pump','Color','k')
grid on
%matlab2tikz('JPinWell.tikz', 'height', '\figureheight', 'width', '\figurewidth');
```

F.2 Compressible Equations

F.2.1 Jet Pump Program

```
% PROGRAM THAT CALCULATES THE EXACT VALUES AS PER FUCHS AND PTC

clearvars
clc

X0 = [0.03843,150.*10^5,219.8.*10^5]';

x = fsolve('nleq',X0);

disp('Q2 [m3/s]')
disp(x(1))
disp('Po [bar]')
disp(x(2)/10^5)
disp('Pt [bar]')
disp(x(3)/10^5)
```

F.2.2 Jet Pump Function - nleq

```
function f = nleq(x)
Q1 = 0.03843; % Surface injection rate, m3/s
```

```
Ps = 145.*10^5; % Pump intake pressure, Pa
Pi = 471.5.*10^5; % Power fluid pressure, Pa
Pd = 222.7.*10^5; % Pump discharge pressure, Pa. CONSTRAINT

Kn = 0.05; % Nozzle loss coefficient
Ken = 0.05; % Entry loss coefficient
Kth = 0.15; % Throat loss coefficient
Kdi = 0.15; % Diffuser loss coefficient
An = 0.000154838; % Nozzle area, in^2
Ath = 0.0006451; % Throat area, in^2
rhof = 833; % Density of oil, kg/m3
rhopf = 1015; % Power fluid density, kg/m3
rhog = 107; % Gas density @ 145 bar
phis = 0; % GLR

gamma = rhog./rhopf;
S = rhof./rhopf;
R = An/Ath;
a = 0; % Ath/Ad, a=0 is a reasonable assumption
c = (1-R)/R;

% Jet Dynamic pressure (Z) and Nozzle velocity (Vn)
Z = (Pi-Ps)./(1+Kn);



% [Q2,Po,Pt]
% x(1),x(2),x(3)

%f = @(Po)
%(Q2./Q1).*(Ps-Po)+phis.*Ps.*log(Ps/Po)-Z.*((S.*Q2./Q1+phis.*gamma)./c.^2).
% *(1+Ken).*(Q2./Q1+phis.*Ps./Po)^2;...
f(1) = (x(1)./Q1).*(Ps-x(2))+phis.*Ps.*log(Ps/x(2))- ...
Z.*((S.*x(1)./Q1+phis.*gamma)./c.^2).*(1+Ken).*(x(1)./Q1+phis.*Ps./x(2))^2;

%g = @(Pt)
%(Po-Pt)-Z.*R.^2*(2+Kth)*(1+S.*Q2/Q1+gamma.*phis).*(1+Q2/Q1+phis.*Ps/Pt)
%+2.*Z.*R+2.*Z.*R^2.*(S.*Q2/Q1+gamma.*phis).*(Q2/Q1+phis.*Ps/Po)/(1-R);
f(2) = (x(2)-x(3))-Z.*R.^2*(2+Kth)*(1+S.*x(1)/Q1+gamma.*phis).*(1+x(1)/Q1+ ...
phis.*Ps/x(3))+2.*Z.*R+...
2.*Z.*R^2.*(S.*x(1)/Q1+gamma.*phis).*(x(1)/Q1+phis.*Ps/x(2))/(1-R);

%h = @(Pd)
%(Pd-Pt)+phis.*Ps.*log(Pd/Pt)/(1+Q2./Q1)-Z.*R^2.*
%((1+S.*Q2./Q1+phis.*gamma)/(1+Q2./Q1)).*((1+Q2./Q1+phis.*Ps/Pt)^2-
%a^2.*(1+Q2./Q1+phis.*Ps/Pd)^2-Kdi.*(1+Q2./Q1+phis.*Ps/Pt)^2);
f(3) = (Pd-x(3))+phis.*Ps.*log(Pd/x(3))/(1+x(1)./Q1)-...
Z.*R^2.*((1+S.*x(1)./Q1+phis.*gamma)/(1+x(1)./Q1)).*...
((1+x(1)./Q1+phis.*Ps/x(2))^2-a^2.*(1+x(1)./Q1+phis.*Ps/Pd)^2-...
```

```
Kdi.*(1+x(1)./Q1+phis.*Ps/x(2))^2);

end
```